



Seismic strengthening of existing RC buildings with external cross-laminated timber (CLT) walls hosting an integrated energetic and architectural renovation

Lorenzo Badini^{1,2} · Stephan Ott¹ · Patrik Aondio¹ · Stefan Winter¹

Received: 10 December 2021 / Accepted: 7 April 2022 / Published online: 7 June 2022
© The Author(s) 2022

Abstract

In this study a timber-based integrated solution is presented to solve at once common issues affecting typical reinforced concrete (RC) existing buildings, such as seismic and energy performances, providing an eco-friendly alternative to steel external bracing systems. Cross-laminated timber (CLT) walls are provided perpendicularly to the external façades as strengthening elements while interposed CLT slabs are foreseen at each floor level to host new architectural units together with a new envelope. While the connections to the foundations and to the existing RC frames are provided respectively with steel brackets and axial-connectors distributed along the height of the building, a post-tensioned connection, between CLT panels (PT-CLT connection), is implemented in the system to guarantee resistance to horizontal actions acting parallel to existing façades with consequent structural independence and architectural freedom. On this regards a first look at the findings of an experimental campaign carried on the Technical University of Munich are presented. A numerical model is developed with finite element software characterizing each type of connector for linear and non-linear analyses. Modal analyses with response spectrum are performed to verify structural elements and connectors, while pushover analyses with target displacement checks are performed to assess the obtained seismic improvement. Finally, the preassembled architectural components that allow to renovate the envelope and the provided assembly procedure are revealed.

Keywords Cross-laminated timber · Existing building · Seismic retrofit · Target displacement · Energy retrofit · Numerical analyses

1 Introduction

The renovation of existing building stock is an increasingly important topic, due to the progressive deterioration of the major part of the buildings, designed and realized between the 50's and the 90's. The European Union counts about 200 million existing units, representing around 27% of total energy consumption (Ferrante et al. 2018). Furthermore,

✉ Patrik Aondio
aondio@tum.de

Extended author information available on the last page of the article

many of these are located in seismically active areas and designed without any reference to horizontal loads or follow outdated standards. This is the main context of Pro-GET-onE research and innovation project, whose main objective is the design, verification and assessment of an integrated technological system to be assembled externally to existing reinforced concrete (RC) structures in order to obtain a seismic and energy improvement that at the same time offers additional space for extended housing units (Ferrante et al. 2018). The structural seismic improvement has been proven with a steel three-dimensional exoskeleton applied on a five-storey student house (Badini et al. 2019; Fotopoulou et al. 2018). Seismic analyses have been performed through FEM software before and after the application, to existing RC structures, of the strengthening steel-based exoskeleton, showing that the increase in strength and stiffness of the entire building is usually associated with an increase in capacity and a reduction of displacements. The contribution in terms of strength provided by the external strengthening structures has been found to be most effective for weak existing structure, characterised by slender bearing members and large displacements. For stronger structures, excessive bracing may lead to high stresses on the existing elements, not always involving favourable outcomes in terms of reduction of required ductility. In addition, a specific distribution of stiffness in the external structures may reduce or avoid pre-existing torsional effects in the primary vibrating modes, further increasing the possible benefits. Complementary to the external structure, architectural components are developed for the extensions of the building envelope (Ferrante et al. 2018; Fotopoulou et al. 2019; Ott and Krechel 2018). The pre-assembled solutions had to face the challenges of architecture variability (extra-room, sunspace, and balcony), completing the strengthening structure, and were provided as prefabricated boxes or slabs composed by combinations of cross laminated timber (CLT) panels and wooden frames. Together with the increased space delivered by the extension of the exoskeleton, airtightness, insulation, and new façade is provided by the components. These interventions result in higher energy efficiency, renewal of the building envelope, thus updated asset value (Ferrante et al. 2018). Combined with new and efficient heat, ventilation, and air conditioning (HVAC) systems, their piping, and the inclusion of renewable energy sources (RES) on the roof, the architectural components aim to achieve the level of nearly zero energy building (Assimakopoulos et al. 2018; Barmpareosos et al. 2019; Ferrante et al. 2019). Worth mentioning are also the contributions that address the environmental impact of the project (Luca Guardigli et al. 2019a; Guardigli et al. 2019b), comparing different scenarios within the prototype-renovation and against the process of demolition and rebuild. From the LCA it is calculated that over a period of analysis of 50 years, out of a total of about 700 tonnes of CO_{2e} related to the whole renovation, 35% is due to the external steel structure. It is clear that to further address climate change mitigation and minimise the environmental impact, alternative structural solutions should be investigated.

In the last decades, as consequence of an accelerated drive towards sustainable materials, the rediscovery of wood as a structural material has led to the spread of new engineering wood products and related research (citing only mass timber products, laminated veneer and strand lumber and cross-laminated timber). In particular, CLT panels are produced to a high degree of prefabrication which allows efficient and safe on-site installation and they have been applied globally in many low-rise and mid-rise buildings typically using platform construction technology (Dangel 2018). Under seismic loads, CLT shear walls with properly designed connection systems are able to provide adequate lateral capacity for multi-storey buildings. Despite the lightness of the material which allows to have low values of mass, a higher level of lateral in-plane strength and stiffness can be reached (Dujic et al. 2008). These qualities make it a product that is easily applicable for extensions

(Hristovski et al. 2018; Iztok Sustersic et al. 2010) or renovation of existing buildings (Margani et al. 2020; Mora et al. 2015; Stazi et al. 2019; Iztok Sustersic and Dujic 2012, 2013, 2014a; Sustersic and Dujic 2014b). In Slovenia, Sustersic I. and Dujic B. evaluated a new system for combined seismic retrofit and energy efficiency that exploited the CLT panels applied in parallel to the façades of an existing RC-building (Sustersic and Dujic 2012). The CLT jacket, depending on the dimensions of the applied panels, reveals itself as a not invasive intervention that is rigidly connected to the RC frames by means of angular brackets nailed to the wood and fixed with bolts to the concrete slabs. It proved to increase stiffness and strength of the entire existing RC structure without influencing the global ductility. Furthermore, the CLT panels can be upgraded with various insulation types implying an integrated energetic renovation. The same system was then developed and optimised on RC frames and in combination with masonry unreinforced structures, where through the variation of the bonding system or the connectors, an increase in ductility was provided. Furthermore, the system has demonstrated the possibility of increasing the performance of already severely damaged structures (Sustersic and Dujic 2013, 2014a, b). In this context, from the University of Venice (IUAV), studies were conducted in order to characterise layering configurations applied on CLT-strengthening panels, taking into account minimisation of heat-losses, environmental impacts and intervention costs (Mora et al. 2015). More recently, a similar solution has been proposed in (Margani et al. 2020) that foresees again an outer shell made of CLT panels combined with an insulation layer within additional timber framework. Simulations on the system have demonstrated the reduction on energy demand, technical details are aimed at developing a pre-assembled system that can be easily assembled from the outside with dry components, exploiting a new friction-based dissipative connection between the panels and the RC frames. Finally, confined and unconfined CLT panels were studied also as new infills for RC frames showing a substantial reduction in lateral displacement complemented by higher peak load capacity (Stazi et al. 2019).

The study presented in this article will describe an innovative and integrated system that together with energetic and structural improvements, entails the possibility of increasing the volume of the existing residential units, thereby increasing the value of the real estate and further mitigating renovation costs. In fact, the addition of living space as an extension on the existing perimeter of residential stock can be a significant parameter for the large-scale exploitation of the system. Although there are clear logistical and legislative limitations, as not all buildings that could benefit from this system have the possibility to use the space in front of the façades, and often local regulations have strict requirements for renovations, paying attention to equally important structural aspects such as the increase of storey masses and the effects on the distribution of stresses on existing and new lateral resisting elements, the integrated system could stimulate stakeholders, owners and inhabitants to renovate their buildings and thus boosting the benefits on the impacts of energy consumption and safety of the European building stock.

2 Integrated system

In accordance with the philosophy of the EU project, it was necessary to develop an integrated system capable of satisfying all the three principal objectives (seismic safety, energetic improvement, and additional space). By means of external performing façades or



Fig. 1 a Photo of the precast-concrete walls case study in Brasov (Google LLC 2022); b Typical plan of the case study including the architectural renovation provided for the internal partitions (Maslaev Consulting 2015)

extensions, prefabricated wooden components can easily be installed with effective results (Lattke et al. 2011; Pihelo et al. 2017).

Within the contents of Pro-GET-onE three case studies are provided: a moment-resisting RC frame located in Athens (Greece), a hybrid masonry-RC structure in Bagnolo in Piano (Italy), a precast concrete walls structure in Brasov (Romania). The latter has been chosen as reference structure due to the climatic conditions of the area, and the local availability of wood. It is a five-stories homeless dormitory built in 1972, characterised by a superstructure made of prefabricated RC walls (Fig. 1a). More information about this case study is reported in (Maslaev Consulting 2015; Pro-GET-onE Consortium 2018). In

the reports it is highlighted that the energy performance is poor with reference to winter consumptions and domestic hot water production and that an architectural renovation is required due to the change of use to social housing block of flats (Fig. 1b). This contrasts with a general good performance concerning the seismic vulnerability assessment. Three indicators are reported with as many procedures: a qualitative assessment based on tables, assessment of the degradation stage from visual and detailed examinations and quantitative assessment based on static linear analysis and capacity/demand ratios for each wall at the base level. Based on the result of the latter, the report states that the building suffers moderate vulnerability and that the structural intervention to consolidate it is not necessary. For this reason, the integrated timber-based system was developed as architectural independent extension for the case study, providing a complete energy renovation of the envelope. A virtual moment-resisting RC structure designed for vertical loads only and with a morphology as close as possible to the Romanian case study (considering spanning changes due to a different structural system) was then numerically investigated in combination with the timber-based strengthening system to prove the seismic improvement. All the data related to the RC frames are reported in chapter 3 as description of the initial state FEM model (Fig. 17).

In order to describe the timber-based extension, after an introduction of the main structural components (slabs and walls), the current chapter introduces the connections provided between the horizontal and vertical CLT panels, between the panels and their foundations, between the panels and the existing RC members and concludes with remarks on possible foundation systems. Due to the complete absence of information on the existing foundations of the real case study and considering that the seismic improvement is evaluated on a fictitious RC moment-resisting structure, specific calculations and details were not carried out for the project. Furthermore, it is important to mention that at the current state of the research project, the fire protection of the whole system was not considered for the design of the structural components and some considerations are only given in chapter 5. Materials, structural elements and connections introduced and described in this chapter are subsequently entered in the finite element software on the basis of what is described in chapter 3.

CLT walls constitute the structural strengthening system for the existing structure and are externally added in continuity of the RC frames, in the plane perpendicular to the external façades. They improve the seismic performance increasing the global stiffness of the system, reducing the displacement demand, and increasing the capacity by avoiding concentration of damages in the lower levels. CLT slabs are then provided horizontally creating a “bookshelf” in which the different architectural solutions are provided, guaranteeing the new performing envelopes (Fig. 2). While the vertical walls are made of 200 mm thick CLT panels composed of five layers of birch (40 – 40 – 40 – 40 – 40 mm) (Jeitler et al. 2016), the slabs are made of 160 mm CLT spruce panels with five layers (40 – 20 – 40 – 20 – 40 mm) and are connected at each floor by means of a moment-resisting post-tensioned connection that adapts the analytical behaviour presented by Wanninger and Frangi (2014, 2016). The strength values of the timber CLT are summarised in Table 1.

Both the connections to the foundations and to the existing structures are made with consolidated and simplified solutions in order to minimise the uncertainties on the numerical analyses and leaving space for further research development. Every wall has been connected to the foundation level with 12 angular brackets (BMF116) and 16 hold-downs (HTT22), distributed on both side of the 2 m width CLT panels. The connection with the existing structure is designed to transmit only the axial loads acting in direction

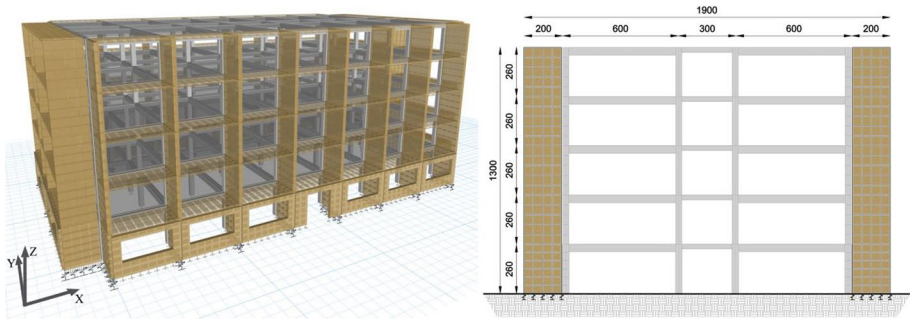


Fig. 2 Finite element model of the cross-laminated timber strengthening system applied to four sides of the building: perspective view and dimensioned vertical cross-section

Table 1 Characteristic strength and stiffness properties in MPa for cross-laminated timber (CLT)-Spruce (European technical assessment document, ETA-06/0009 – EN 338) and CLT-Birch (Jeitler et al. 2016), plus relative mean density values in kg/m³

Value	Units	CLT-Spruce	CLT-Birch
$f_{m,CLT,k}$	MPa	24	38
$f_{c,0,CLT,k}$	MPa	21	38
$f_{c,90,CLT,k}$	MPa	2.5	5.0
$f_{t,0,CLT,k}$	MPa	14	28.5
$E_{0,CLT,mean}$	MPa	12'000	15'000
$E_{90,CLT,mean}$	MPa	370	650
$G_{CLT,mean}$	MPa	690	710
$\rho_{CLT,mean}$	kg/m ³	470	620

perpendicular to the existing façade, allowing the interaction between the two structures only for horizontal actions acting in-plane to the CLT walls.

2.1 PT-CLT connections

Adapting concepts and principles originally developed for precast concrete construction (Priestley et al. 1999), post-tensioned (PT) timber systems have been developed and tested since 2005 at the University of Canterbury (Palermo et al. 2005). The technology takes advantage of unbonded post-tensioned steel tendons passing through internal cavities in timber beams or walls to create a moment resisting connection (Fig. 3a). The seismic demand is satisfied through controlled rocking between structural elements and tendon elongation, which also ensures recentering capabilities. Thus, energy-dissipation devices (replaceable mild steel components, viscous or friction dampers) could be provided creating hybrid connections characterised by the typical flag-shaped behavioural law (see Fig. 3b). For the sake of brevity a complete state of the art on Pre-Lam technology is not summarised here, but reference is made to (Granello et al. 2020).

As mentioned in the previous section, direct reference to the analytical method reported in (Wanninger and Frangi 2014, 2016) was made for the adaptation of the PT connection to CLT panels. With difference from the New Zealand experience, at the ETH Zurich the PT frames are developed with glulam made from Norway spruce, and

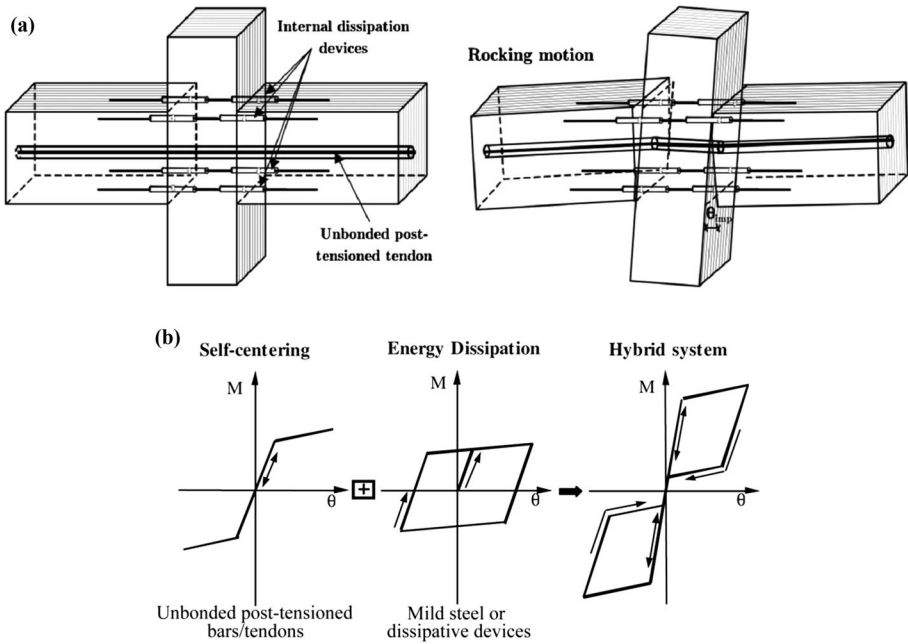


Fig. 3 **a** Schemes of the application of the hybrid concept to laminated veneer lumber frame systems by Palermo et al. (2005): while the unbonded tendon provides moment strength and a recentering behaviour, mild-steel bars allow energy to be dissipated through their deformation. Despite the fact that shear forces are theoretically transferred through the friction generated by the precompression at the interface, in practical applications researchers have often provided corbels, notches or grooves; **b** The resulting idealised flag-shaped hysteresis cycle (Palermo et al. 2005)

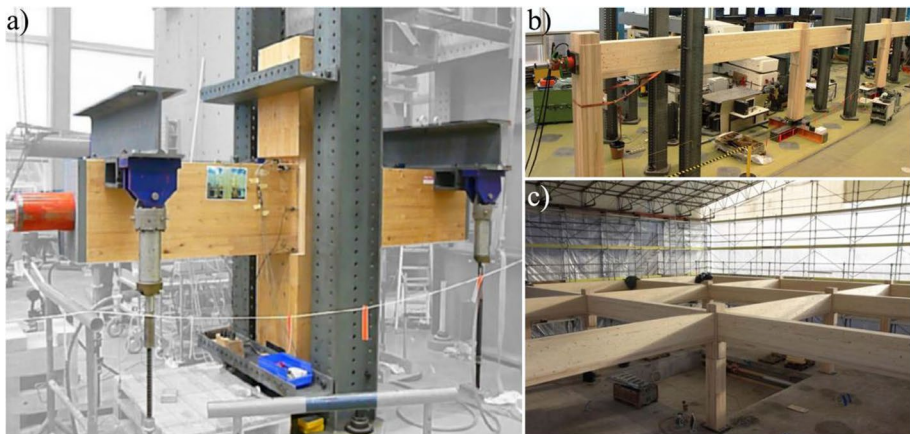


Fig. 4 **a** Glulam column-beam specimen (Wanninger 2015); **b** Three-spans post-tensioned glulam frame (Wanninger 2015); **c** First elevation of the ETH House of Natural Resources (Wanninger 2015)

present a reinforcement made of European ash where high stresses perpendicular to grain occur (column and bottom side of the beams), avoiding the use of steel reinforcements in the joints. Extensive experimental testing have been performed under both gravity and lateral loads, on single column-beam subassemblies, an entire three-spans frame and ending with the construction of a prototype (Wanninger 2015) (Fig. 4).

The analytical model is based on springs that represent the softer column and only bear compressive forces. The beam ends at the interface and behave like a rigid body due to the higher strength and stiffness of the timber components in parallel to grain direction. Hence, the model corresponds to a (stiff) foundation on (soft) ground (Winkler theory) (Wanninger and Frangi 2014). Since there are no dissipating elements, a gap occurs in the interface as soon as there is no compression at either the top or bottom edge of the connection. The analytical model describes the behaviour of the connection (moment-rotation), and based on equilibrium of forces and bending moments at the interface, leads to three stages that depend on the value of the neutral axis x (Fig. 8) (Wanninger 2017; Wanninger and Frangi 2014):

1. Before decompression ($x = h$); the beam is in full contact with the column. Linear behaviour.
2. After decompression ($x < h$); a gap occurs at the edge of the beam. Non-linear behaviour.

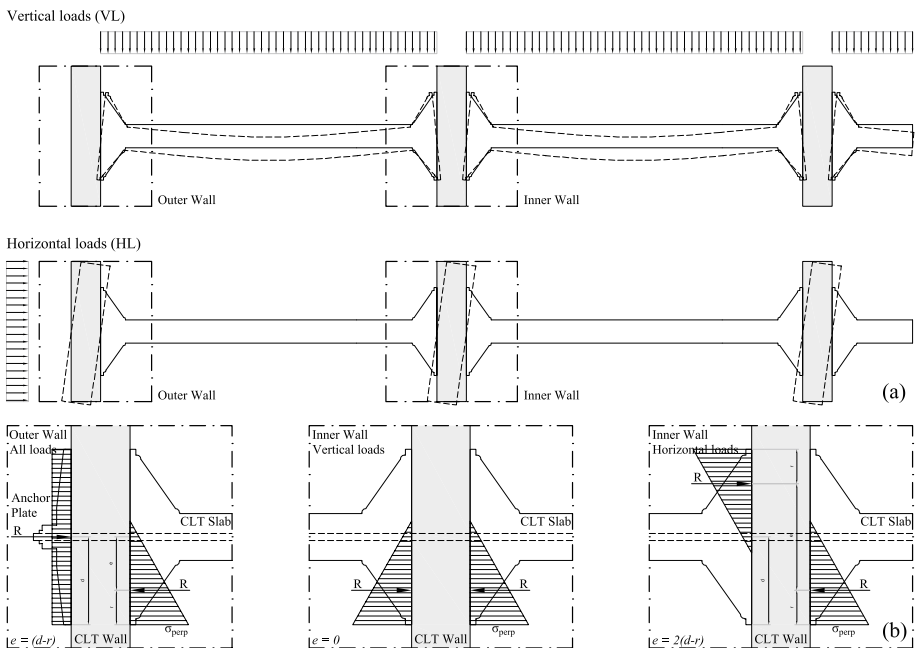


Fig. 5 **a** Identification of outer and inner connections with indication of deformations at the interface according to vertical and horizontal load cases (VL, HL); **b** Distribution of stresses at the connection interfaces of outer and inner walls in the cases of VL and HL

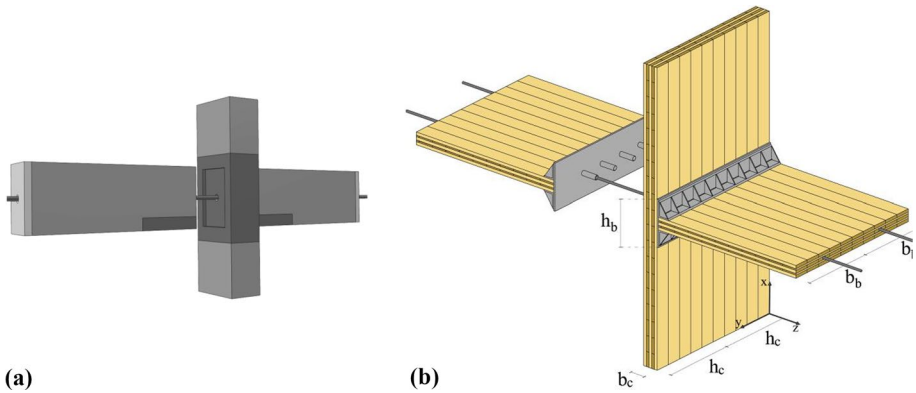


Fig. 6 **a** Three-dimensional view of the post-tensioned timber connection developed at ETH Zurich (Waninger 2015); **b** Proposed post-tensioned connection between cross-laminated timber panels by means of steel unbonded cables and composed plates enlarging the contact interface

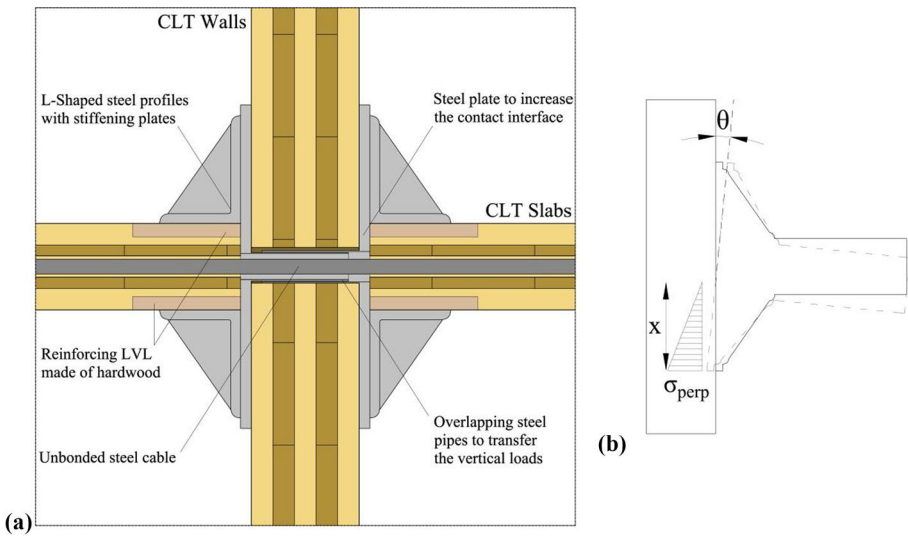


Fig. 7 **a** Detail of the post-tensioned cross-laminated timber connection with steel composed plates; **b** Schematic representation of the values resulting from the analytical model (rotation θ , stresses perpendicular to grain in the vertical element σ_{perp} and, neutral axis x)

3. Tendon elongation ($x < h/2$); when the neutral axis goes below the tendon, the latter gets elongated, resulting in an increase in tendon force and stiffness. Non-linear behaviour with increased slope.

Asymmetrical loads imply shear deformations in the column that depend on the eccentricity of the resultant compressive forces on the two interfaces of the joints. This occurs in the outer joints and more significantly in the inner ones when subject to horizontal loads as shown in Fig. 5 with reference to the adapted solution based on CLT panels.

Table 2 Comparison between the values used in (Wanninger and Frangi 2014), referring to a column specimen made of ash, and the vertical cross-laminated timber element made of birch with reference to half of the total depth. These inputs were used for the calculation of the rotational behaviour as described in (Wanninger and Frangi 2014)

Value	Units	D40 (Wanninger and Frangi 2014)	CLT-Birch (Fig. 6 and Table 1)
$E_{90,mean}$	MPa	860	650
$G_{0,mean}$	MPa	810	–
S_{xz}/b_c	MPa	–	246
$f_{c,90,k}$	MPa	8.3	5
b_c	mm	280	200
h_c	mm	600	1000
b_b	mm	400	1000
h_b	mm	600	600

The transition from a beam-column system with linear elements to a system with two-dimensional elements involved the use of a composite steel plate to increase the contact surface between horizontal and vertical elements maintaining adequate rotational stiffness (depending on the height of the horizontal element) without encountering a premature failure of the grain compressed perpendicularly (Fig. 6).

This connection steel plate is composed by a large steel plate (600×2000 mm) 20 mm thick, with two angular brackets L 200×150×18 mm and four steel pipes (Fig. 7a). The large plate with the L-profiles allows to increase the height of the horizontal element for the evaluation of the rotational behaviour while the steel tubular profiles are inserted in specific holes of the CLT vertical element to transfer the vertical loads. The holes in the CLT provide tolerances allowing a relative rotation of the plate, and the steel pipes must overlap one another during the assembly of inner joints ($\phi 48.3 \times 2.6$ mm and $\phi 60 \times 2.16$ mm). Reinforcing LVL made of hardwood is provided at the contact interface between the horizontal CLT element and the smaller side of the angular steel profile to avoid the crushing of the grain. Alternatively, a stiffer external layer could be already provided manufacturing the CLT slabs. The steel unbonded tendon passes through the horizontal elements along their development and across the vertical one. It is composed by four wired strands with cross sectional area about 600 mm², Young's modulus of 197 GPa and a maximal tension strength about 1770 MPa (ETA-13/0810 in (BBV Systems 2021)).

In order to consider the PT-connection for the seismic analysis, the analytical model presented in (Wanninger and Frangi 2014, 2016) was adapted and used to plot the rotational behaviour at the connection interface. Table 2 shows the input data used by the analytical model for the calculation of the rotational spring characterizing the PT-connections. Figure 6a is showing the PT connection made with linear glulam elements (Wanninger and Frangi 2014), while Fig. 6b represents the adaptation to two-dimensional CLT elements through the use of steel plates to maintain adequate rotational stiffness and avoid premature grain crushing in the vertical elements. The latter also illustrates the notations shown in Table 2. In order to apply prestressing to the CLT slabs and to create the moment-resisting connection at the interface with the CLT walls, two tendons are provided within the 2 m depth of the timber-based portals. The geometric dimensions for the calculation of the rotational springs are therefore related to half of the depth CLT portals, the presence of a tendon and the mechanical characteristics of the vertical birch CLT walls. In addition to the modulus of elasticity in the direction perpendicular to the grain, which is essential for obtaining the modulus of subgrade reaction (Wanninger 2015) to account for the bedding

Table 3 Formulations to determine the rotational behavior of the post-tensioned cross-laminated timber connection. Reference is made to the analytical model proposed in Wanninger and Frangi (2014)

Before decompression ($x = h_b$)	After decompression ($x < h_b$)	Tendon elongation ($x < h_b/2$)
$c = \frac{E_{90} \cdot \sigma_2}{b_c}$	$M_{dec} = P_0 \cdot \frac{h_b}{6}$	$M_{t,el} = P_0 \cdot \frac{h_b}{3}$
$\theta = \frac{\sigma_1 - \sigma_2}{c} \cdot \frac{1}{x}$ (1)	$x = 3 \cdot \left(\frac{h_b}{2} - \frac{M}{P_0} \right)$ (8)	$x = 3 \cdot \left(\frac{h_b}{2} - \frac{M}{P} \right)$ (14)
$M = c \cdot \frac{b \cdot h_b^3}{12} \cdot \theta$ (2)	$\theta = \frac{\sigma_1}{c} \cdot \frac{1}{x}$ (9)	$\Delta L_p = \theta \cdot (d - x)$ (15)
$\sigma_{1,2} = \frac{P_0}{A} \pm \frac{M}{W} = \frac{P_0}{b \cdot h_b} + \frac{M}{\frac{b \cdot h_b^2}{6}}$ (3)	$M = P_0 \cdot \left(\frac{h_b}{2} - \sqrt{\frac{2}{9} \cdot \frac{P_0}{b \cdot c \cdot \theta}} \right)$ (10)	$P = P_0 + A_p \cdot E_p \cdot \frac{\theta \cdot (d-x)}{L_p}$ (16)
$r = h_b - \frac{\sigma_2 \cdot \frac{h_b^2}{2} + (\sigma_1 - \sigma_2) \cdot \frac{h_b^3}{3}}{\sigma_2 \cdot h_b + (\sigma_1 - \sigma_2) \cdot \frac{h_b}{2}}$ (4)	$\sigma_1 = \frac{2P_0}{3 \cdot b \cdot \left(\frac{h_b}{2} - \frac{M}{P_0} \right)}$ (11)	
$\gamma = \frac{R}{\frac{S_{xz}}{h_c} \cdot A_c}$ (5)	$r = \frac{x}{3}$ (12)	
$\theta_{GA} = \frac{\gamma - e}{h_b} = \frac{R}{\frac{S_{xz}}{h_c} \cdot A_c} \cdot \frac{e}{h_b}$ (6)	$\theta_{GA} = \frac{R}{S_{xz} \cdot h_c} \cdot \frac{e}{h_b}$ (13)	
$R = P$ (7)		
x neutral axis depth	R resultant force	
h_b height horizontal element	A_c cross sectional area vertical element	
c spring constant	e eccentricity	
b_c width vertical element	θ_{GA} rotation due to shear deformation	
E_{90} Young's modulus perpendicular to grain	S_{xz} shear rigidity of the CLT	
θ rotation	h_c height vertical element	
$\sigma_{1,2}$ stresses at the bottom and top interfaces	ΔL_p elongation of the tendon	
M moment	d position of the tendon	
b width horizontal element (b_b)	P increased tendon force	
P_0 initial tendon force	L_p length tendon	
r position resulting force	A_p cross sectional area of the tendon	
γ shear angle	E_p modulus of elasticity of the tendon	

springs at the interface of the horizontal elements to the vertical ones, the shear modulus was also required to include the additional joint deformations due to eccentric loads. Due to the different mechanics of cross-laminated timber from solid wood, the shear modulus G of the latter is compared with S_{xz}/b_c , with S_{xz} representing the shear rigidity of CLT in the xz plan, as calculated in (Aondio et al. 2020b).

Through the adaptation of the analytical model, it was possible to obtain the laws describing moment, compression perpendicular to grain in the vertical element, neutral axis position and tension in the tendon in relation to the rotation at the interface. With reference to the analytical model introduced in (Wanninger and Frangi 2014, 2016), the equations reported in Table 3 were used to determine the rotational behaviour of the PT-CLT connections for the three main phases introduced above (before, after decompression and after tendon elongation). As mentioned above, the analytical model is based on springs, which have a constant c (Table 3) defined as the ratio between the compressive stress from the uniform load and the displacements due to the applied loads. The equilibrium of forces and bending moments at the interfaces leads to equations for the moments (2, 10), the rotation (1, 9) and the neutral axis depth (8, 14). The calculated compressive stresses are calculated on the basis of the linear elastic theory, thus neglecting edging effects (stress concentrations) and the softening behaviour of the wood components (Fig. 7b). The second phase begins when the decompression moment is reached and the stresses at the top edge of the interface result are zero. In this phase

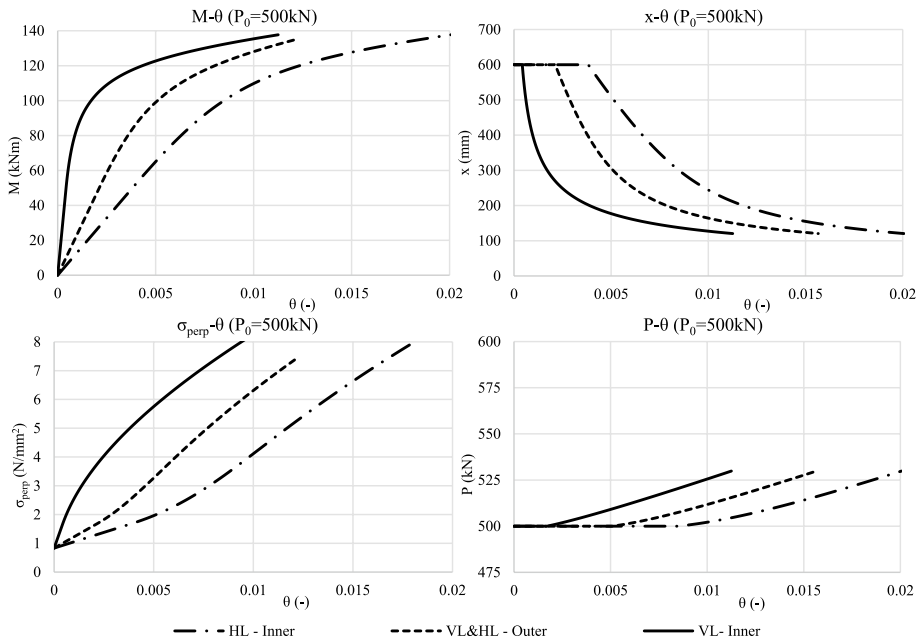
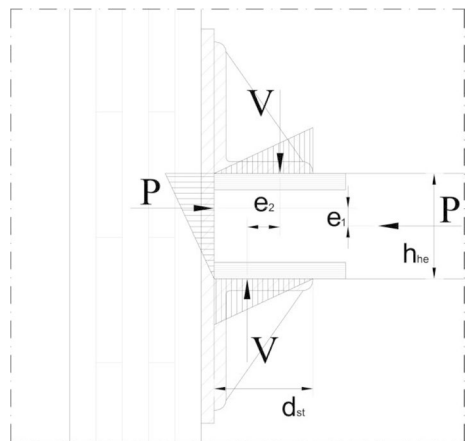


Fig. 8 Moment-rotation behaviour, compression perpendicular to grain, neutral axis position and tension in the tendon in relation to the rotation at the interface of the post-tensioned cross-laminated timber connection, calculated for the inner elements with vertical loads (VL) and horizontal loads (HL) and for the outer elements

the neutral axis decreases as the applied forces increase. Finally, when the neutral axis reaches the central position of the tendon, the latter is elongated, and its force increased. Using the Hooke’s law, and as the tendon force has become a function of the rotation and the depth of the neutral axis, an iterative procedure is required to obtain a solution.

Fig. 9 Forces and stresses affecting the end of the horizontal cross-laminated timber panel



The analytical model was implemented in a spreadsheet script and, after calibrating it with input and results provided in (Wanninger and Frangi 2014, 2016), it was used to plot the behaviour of the PT-CLT connection presented in this study.

Below in Fig. 8 the relationships mentioned above are shown with reference to half of the depth of the system (1 m with one steel cable) and an initial tension (P_0) set to 500 kN. It is evident how much relevant is the shear deformation of the CLT vertical element on the rotational stiffness due to the lower value S_{xz}/b_c compared to $G_{0,mean}$ from (Wanninger and Frangi 2014).

Finally, it is important to mention that the analytical model developed in (Wanninger and Frangi 2014) was particularly precise until the phase of tendon elongation. In this phase the analytical model was losing precision, overestimating the stiffness and implying the use of an experimental factor to correct the spring stiffness of the analytical model at the beginning of the tendon elongation (Wanninger and Frangi 2014). However, for the purpose of this study, the connection between CLT components is meant to stay in the elastic range under the design seismic loads. Thus, allowing the exploitation of the analytical model without experimental coefficients.

The failure of the connection is related to the crushing of the grain. From the graphs in Fig. 8 it is possible to identify the rotation which corresponds to a compression perpendicular to the grain of the vertical element, which for birch is fixed at 5 MPa. In addition, with the equilibrium between the moment at the interface and the prestressing force P it is also possible to determine the force V that defines the stresses at the interface between the steel angle brackets and the pieces of LVL reinforcement, as shown in Fig. 9. By estimating the stresses at the interfaces, it was possible to verify the connection against the design loads. A mechanical fixation of the LVL layers to the horizontal element of the CLT would also allow these elements to be replaced in case of major events.

$$M = P \cdot \frac{h_{he}}{6} + V \cdot \frac{d_{st}}{3} \tag{17}$$

$$V = \left(M - \frac{P \cdot h_{he}}{6} \right) \frac{3}{d_{st}} \tag{18}$$

$$\sigma_{perp,LVL} = \frac{2V}{d_{st} \cdot b_b} \tag{19}$$

A specific experimental campaign has been performed to prove the adaptation of the analytical model to the CLT element by means of steel plates and will be mentioned here only in its main results. This connection between CLT vertical and horizontal panels has never been used or tested before and could represent an innovative alternative

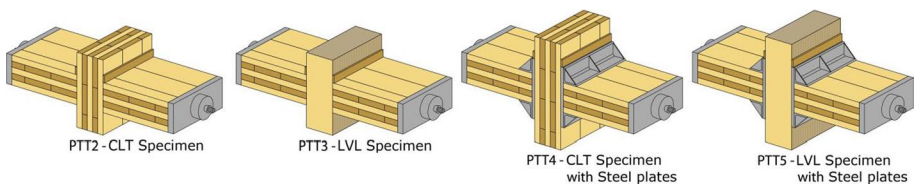


Fig. 10 Axonometric sketches of the different specimens provided for the post-tensioned tests

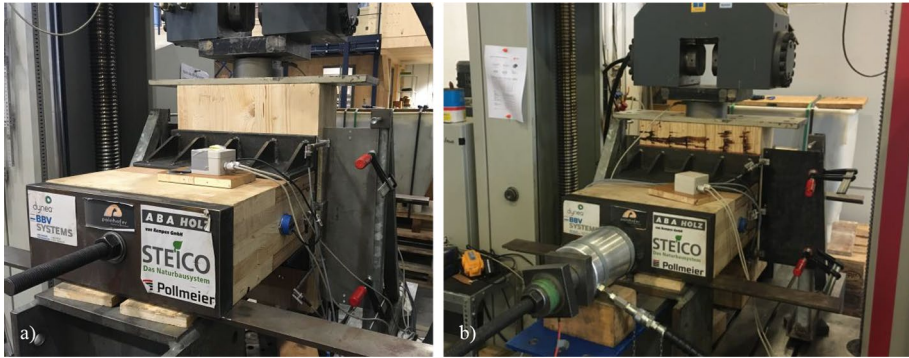


Fig. 11 **a** Photo of the right side of the setup for PTT4; **b** Photo of the left side of the setup for PTT5

to more consolidated connections for this specific structural system or similar structures. The behaviour of CLT vertical walls is already present in literature, together with the use of connectors at the foundation level, such as angular brackets and hold-downs (Dujic et al. 2008, 2010; Gavric et al. 2015; Iztok Sustersic et al. 2016). Therefore, the need for validation of the connection with post-tensioning cables between CLT panels was evident.

The experimental tests were carried out at the material testing laboratory (MPA-BAU) of the Technical University of Munich. Compared to the connection designed for the main strengthening system introduced above, the validation tests were downsized in order to minimise the amount of material required, while maintaining the objective of testing the specimens on a 1:1 scale. Only a part of the connection was analysed by considering elements of the same thickness as those foreseen for the main structure, but reducing the width, the length, and the forces involved (the prestressing forces were reduced as well as the height of the composed steel plates, 400 mm compared to 600 mm). The use of steel plates to enlarge the contact area between the horizontal and vertical elements was foreseen in order to demonstrate the possibility of adopting the above-mentioned analytical system. Therefore, in order to prove the effectiveness of the steel plates for the system and the accuracy of the analytical model to describe the rotational behaviour, different test configurations were investigated, varying the material used for the vertical elements (walls), with and without the provision of the composed steel plates. The specimens are composed of three wooden elements (two representing the floors and one representing the walls), prestressed together by means of an unbonded steel threaded rod (instead of strands, which were preferable but not applicable for safety reasons) passing through the elements. Due to budget limitations, safety constraints, and suppliers' availability, four configurations were tested (Fig. 10).

- PTT2—PT connection test between two horizontal CLT pieces (spruce, C24), connected to a vertical CLT element (spruce, C24) by means of a threaded steel PT rod (prestressing force of 150 kN).
- PTT3—PT connection test between two horizontal CLT pieces (spruce, C24), connected to a vertical LVL-R element by means of a threaded steel PT rod (prestressing force of 220 kN).

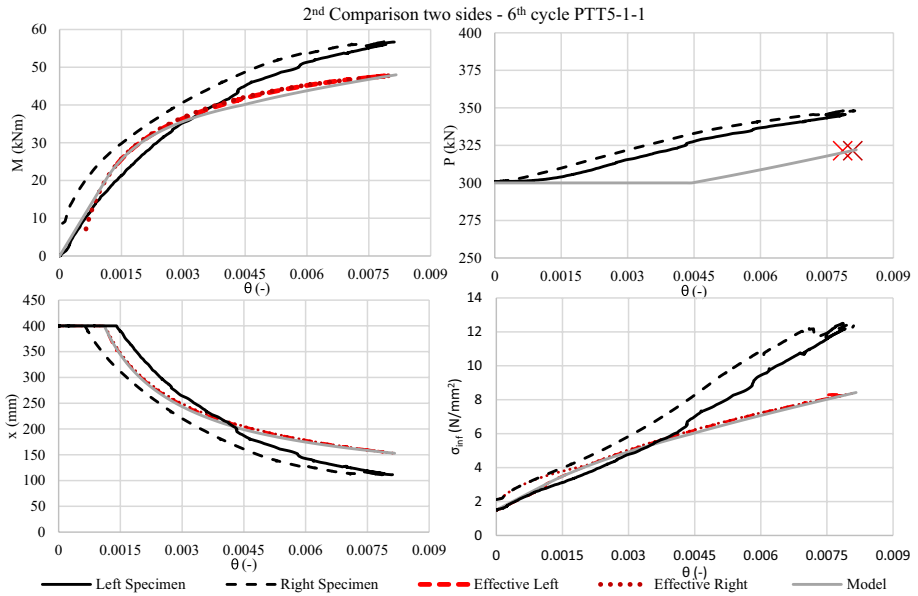


Fig. 12 Evaluation of PTT5-1-1 showing the moment-rotation behaviour, tendon force, stresses at the interface and neutral axis depth proceeding from the left corner in clockwise direction; the grey curves represent the prediction of the analytical model, while the red curves and crosses indicate the influence of the tendon elongation for right and left samples

- PTT4—PT connection test between two horizontal CLT pieces (spruce, C24), connected to a vertical CLT element (spruce, C24) by means of a threaded steel PT rod (prestressing force of 220 kN) and providing an intermediate steel plate to extend the contact interface (Fig. 11a).
- PTT5—PT connection test between two horizontal CLT pieces (spruce, C24), connected to a vertical LVL-R element by means of a threaded steel PT rod (prestressing force of 300 kN) and providing an intermediate steel plate to extend the contact interface (Fig. 11b).

The use of LVL elements as vertical walls was done to provide a more rigid variant to the use of CLT elements in spruce in vertical position. The values of $E_{c,90}$ and $f_{c,90,k}$ of the LVL specimens used for the experimental investigations, in fact, allowed to obtain results comparable to the use of birch CLT elements (solution provided for the main project solution). However, as also specified by the suppliers, the use of LVL elements for an application such as the one proposed for the main project would not be feasible due to higher costs and problems related to creep and swelling of a full-scale wall element.

The tests investigated the behaviour under vertical loads of the PT connection and the setup was designed to minimise the size of the specimens in order to fit the hydraulic drive worktable (Zwick600). Instead of pushing down the horizontal elements (Wanninger and Frangi 2014), the setup provided two supports at the ends of the horizontal elements and the vertical element suspended through the prestressing of the tendon (Fig. 11). The behaviour of the connection was obtained measuring the rotation at the two interfaces of the vertical element while the hydraulic drive pushed it downwards. Other measured parameters

were the vertical force, the prestressing force and the vertical displacement. For each type of test, at least three different samples of a similar vertical element were tested. The wall specimens loaded in combination with the steel composed plates (PTT4 and PTT5) were also tested repeatedly with all cycles, due to the absence of relevant failure in the perpendicularly compressed grain. A total of 29 tests were therefore realised in the testing hall of the TUM. Only the sixth load-cycle of one specimen-type is presented here (Fig. 12), mentioning, however, that consistent behaviour was found for all other tests depending on the most influential parameters (such as initial tendon force, height of the widening steel plates and material). Figure 12 shows the isolated sixth cycle of the PTT5 specimen, moment, tendon force, neutral axis and stresses perpendicular to the grain were plotted in relation to the rotation obtained from the measurements done by lateral transducers and confirmed by additional inclinometers. In all graphs, the results of the analytical model are plotted together with the output of the left and right sides of the specimen. Among the test typologies, PTT5 was chosen since the forces involved were higher and therefore closer to the final solution proposed for the main project (Fig. 8). The influence of the excessive tendon elongation obtained using a short-threaded rod instead of a strand was accounted and removed from the experimental results (red curves and crosses in Fig. 12).

Comparing the different specimens, the following main influences were reported in the experimental campaign: the initial tendon force determined the moment capacity of the connection, the greater the tendon force, the greater the maximum moment of the connection; the presence of the widening plates allowed a greater height to be considered for the horizontal members leading to a substantial increase in stiffness and capacity of the connection; while the mechanical characteristics of the vertical element, that should determine the initial stiffness of the PT-connection, were of minor relevance comparing the results between CLT and LVL-R elements, indicating a behaviour stiffer than expected in the initial loading phase.

The test results show that, in line with the conclusions reported in (Wanninger 2015), the analytical model is conservative (softer) for the PT-connections by adopting low values of initial tendon force and that with the use of the mean elastic moduli in compression perpendicular to the grain (obtained from mechanical tests based on EN408:2012) it was possible to bring the experimental results to convergence for most of the cases. The influence of the threaded rod as an unbounded cable for the test specimens, characterised by a large area and short length, led to an incisive tendon elongation already after the moment of decompression, and not when the neutral axis depth overcomes the position of the tendon. However, the analytical model is shown to be able to predict the behaviour of the PT-CLT connection and to allow the implementation of the moment-rotation behaviour in FEM model. Thus, resulting in a conservative response in terms of moment capacity and initial stiffness, when considering the mean moduli provided by the manufacturers and lower values of tendon forces. The use of steel strands and higher values of tendon forces, although further specific tests are needed, should guarantee the accuracy of the analytical model especially regarding to the first linear phase of the moment-rotation behaviour which is the most relevant part for the seismic analysis. Furthermore, the use of reinforcing layers such as hardwood LVL boards (Fig. 9), or the use of LVL-R specimens (corresponding to any vertical element providing a higher value of compressive strength perpendicular to the grain) has been shown to be effective in avoiding the crushing of the grain and maintain a constant response of the PT-CLT connection during multiple cycles. It is the author's opinion that considering only a stiffer outer layer, e. g. made of hardwood, applied to a spruce CLT wall would be a good and resilience solution, without considering whole CLT hardwood elements (less common, more expensive, and still under investigation). It was,

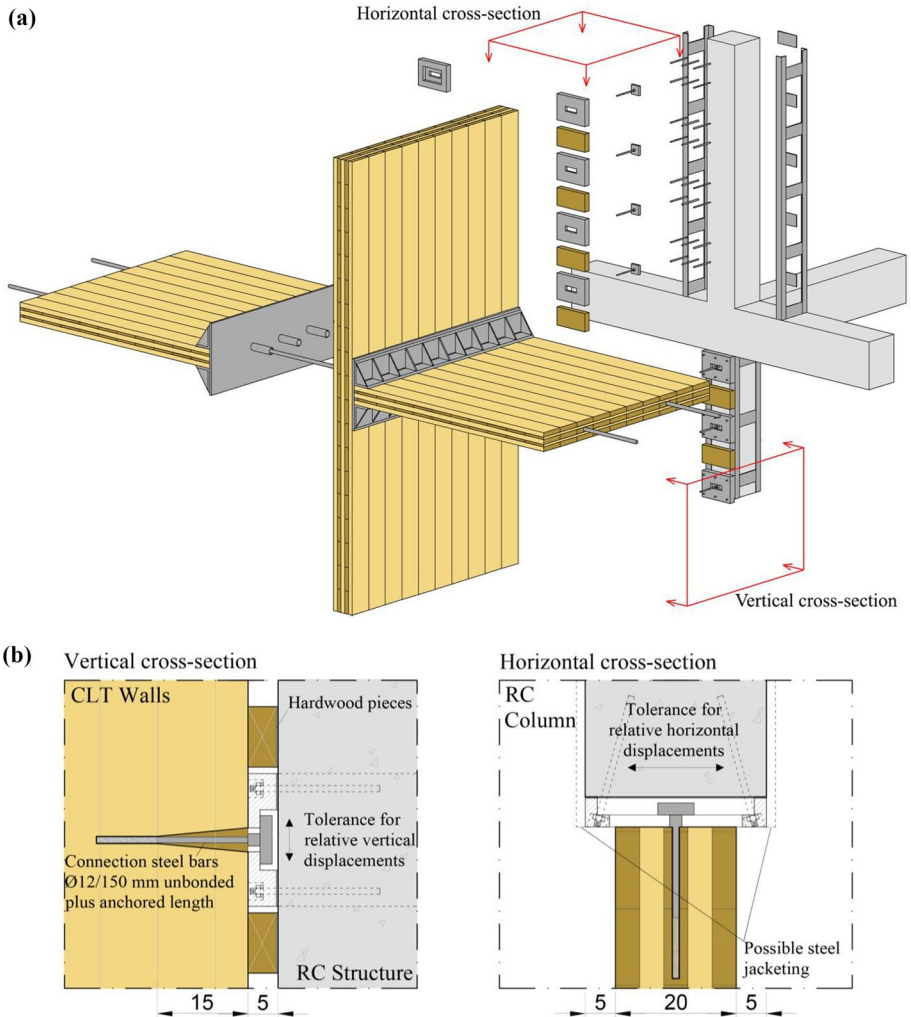


Fig. 13 **a** Axonometric cut-out at typical plan level showing longitudinal post-tensioned connections and axial connections between existing structure and timber-extension. Reference to detail boxes is also given; **b** Sketches of the vertical distributed connection between cross-laminated timber walls and vertical reinforced concrete structural elements (cm as units)

in fact, evident that the stiffness of the connection is strongly dependent on the geometry of the horizontal elements considering the widening plates, more than on the modulus of subgrade reaction. For the main project solution, a steel widening plate with a height of 600 mm was proposed in order to guarantee sufficient stiffness to the whole structure (the widening plates foreseen for the tests had plates with a height of 400 mm), although the capacity and the stresses perpendicular to the grain were too conservative.

In order to optimise the production and effectiveness of wood elements, horizontal elements, as well as vertical elements, could be characterised by an outer hardwood layer in the production stages, as it is already an established strategy of manufacturers to improve

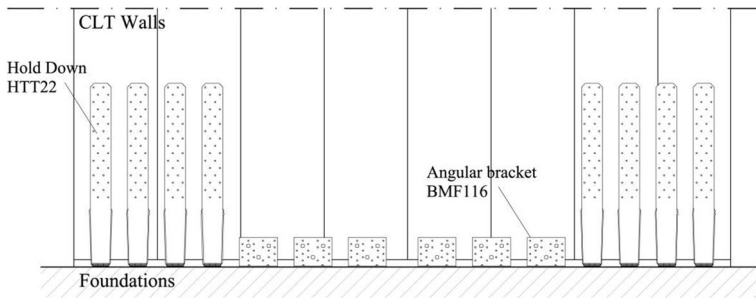


Fig. 14 Multiple connectors at foundation level are represented in the drawing on one side of the cross-laminated timber wall

Table 4 Activated friction forces at the bottom of the inner and outer walls

Value	Units	Inner wall	Outer wall
N	kN	110.3	68.09
F_{fr}	kN	68.4	42.2

structural performance or aesthetics. Alternatively, it would be possible to provide reinforcement boards positioned at the points of greatest compression perpendicular to the grain, and possibly removable and replaceable in the event of major seismic events.

2.2 Connection with the existing structure

As mentioned above, the connection with the existing structure is designed to transmit only axial loads acting in-plane to the CLT walls. Twenty connectors are distributed along the height of the building, consisting of steel rods (ϕ 12/150 mm) fixed with chemical dowels to the CLT walls and providing steel plates to be anchored at the vertical RC elements (Fig. 13). The threaded galvanised rod made of reinforcing steel (B450C) is characterised by a bilinear stress–strain relationship as shown in Fig. 18d. This steel connector plate must provide specific tolerances that allows relative vertical and horizontal displacements. While the relative vertical displacement results in maximum of 5 mm (a tolerance of 10 mm is provided), the horizontal displacement is more significant; considering the roof displacement of the short side (more flexible) under seismic loads, and asynchronous vibration modes, it can reach 100 mm. The fixation of the steel plate to the RC elements is hypothesised from the façade plane with bolts chemically anchored to the RC. Particular attention on this connection must be paid for a realistic application. It is in fact important to have a reliable level of knowledge of the structural existing elements and materials in order to rely on chemical fixations. Additionally, a careful evaluation of the extra loads applied on the columns must be done. Depending on the existing elements, the steel plate may be connected to a steel reinforcing jacketing of the external RC columns to avoid local failures and ensure a safe load transfer. In order to transfer compressive loads between the RC frames and the CLT walls and so avoiding instability in the bars, hardwood components are provided in-between the steel connectors. The local impact of induced external forces on

the existing members, related to poor concrete quality, may imply the need for a parallel internal strengthening strategy aimed at transferring the forces to the RC slabs without damaging the lateral load resisting members. A specific survey should be made for this purpose and drive the selection of the strengthening strategy. In fact, extending the interventions inside the building could jeopardise and/or neglect the benefits of the integrated system, forcing the inhabitants to be relocated in any case.

During the installation procedure the steel bars could be already fixed to the CLT walls and arrive at the construction site with the steel plates in position (hanging from the chemical anchored steel rebars) for the fixation to the RC elements.

2.3 Connectors at foundation level

The use of hold-downs and angular brackets as connectors for CLT structures is widely spread in construction practice and extensively investigated in research (Dujic et al. 2008; Dujic et al. 2010; Gavric et al. 2015; Iztok Sustersic et al. 2016). Due to this reason typical connectors were exploited at the foundation level distributed on both sides of the CLT walls. With specific reference to (Dujic et al. 2010) commercial products already characterised by linear strength properties, secant stiffness and non-linear behavioural laws were provided:

- 12 angular brackets (BMF $90 \times 48 \times 3 \times 116$ mm) fastened to the CLT walls with 12 nails (or screws) $\phi 4 / 60$ mm and with 2 M12 bolts to the foundation were provided in the middle of the walls as shear anchors with a contribution also to prevent up-lift loads (Fig. 14);
- 16 hold-downs (HTT22) fastened to the CLT each with 22 nails (or screws) $\phi 4 / 60$ mm and with 1 M12 bolt to the foundation were placed towards the corners of the walls to resist overturning forces (Fig. 14).

The friction at the foundation level was calculated considering the vertical loads derived from the quasi-permanent load combination. Due to the lightweight of the material and the limited dimensions of the external CLT structure, the axial loads in the walls are limited with a consequent small relevance of the friction at the base. Considering a friction coefficient between wood and concrete of 0.62, the contribution of friction is calculated and exposed below in Table 4.

Despite the rapid implementation of the connectors in the numerical model (Figs. 18d, 20, 21), the right number of them was determined iteratively, checking the force–displacement relationship during non-linear static analysis, matching the seismic global safety of the intervention while keeping the connectors (especially the hold-downs located at the edge of the walls) within their maximum allowed displacement.

2.4 Considerations on foundations

As mentioned above, the foundations of the system introduced in this study were not investigated numerically due to the complete lack of information regarding the existing foundation of the reference structure and its bedding soil. Therefore, there was no information to translate into the fictitious RC moment-resisting structure created to evaluate a possible seismic improvement. This choice, while partially compromising the concreteness of the

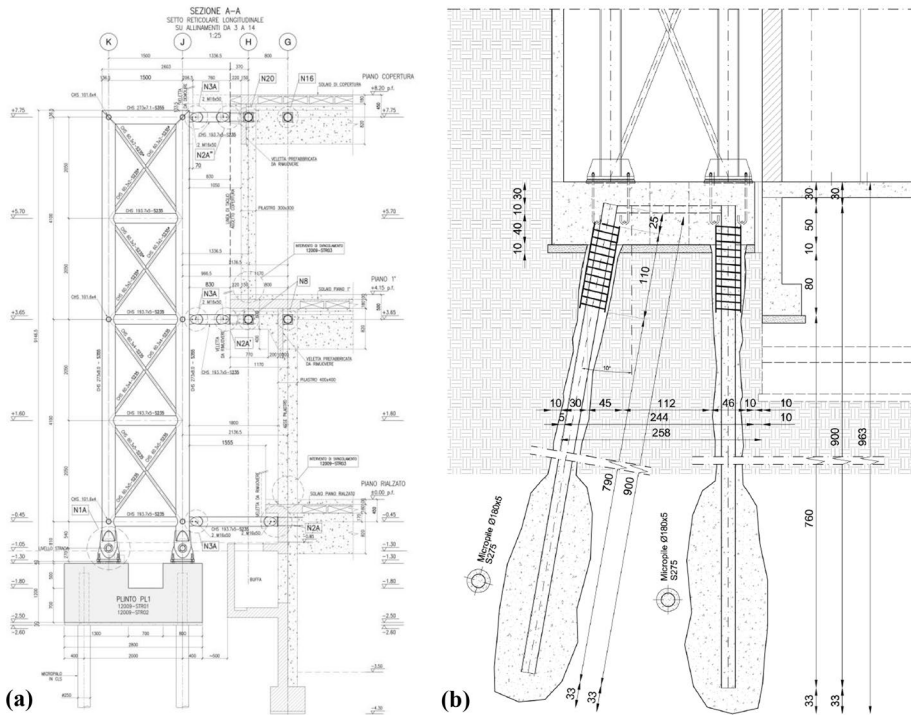


Fig. 15 **a** Technical drawings of the exoskeleton designed by TELEIOS Srl for the seismic retrofit of the office building of Magneti Marelli in Crevalcore (Franceschini et al. 2014); **b** Vertical cross-section detail of the foundation system proposed for the Athens case study

results obtained, allowed us to focus (and isolate) the attention on the two fundamental and most uncertain variables: the post-tensioned connection and the effectiveness of the system to obtain a seismic improvement in areas moderately exposed to seismic hazard. However, on the basis of what was proposed for the preliminary project of the steel exoskeleton (Badini et al. 2019), some considerations can be presented in order to complete the overview of the project and identify its pros and cons.

During seismic events, the external structure responds to the displacements that occur to the existing structure and is therefore pushed and pulled according to the ground motions. This results in high compressive and tensile forces on the foundations that must be properly transferred to the ground. In order to avoid uplift of the exoskeleton, RC piles or micro-piles are usually adopted to deepen the foundation level and transfer the design loads. The deepening of the foundation level first allows to reach soil layers with better quality and strength and is often combined with the construction of bulbs at the base of the micro-piles to increase the contact surface (Fig. 15b). The capacity is then calculated, including both lateral and base contributions, paying attention to the shear forces acting at the pile head which may compromise the effectiveness.

Figure 15a shows a hypothetical solution proposed for the steel exoskeleton applied on another case study of Pro-GET-onE. This solution was discussed among the experts of the project consortium and advisory board of the EU project and follows the experience of the retrofit of the Magneti Marelli office building (Franceschini et al. 2014), illustrated in

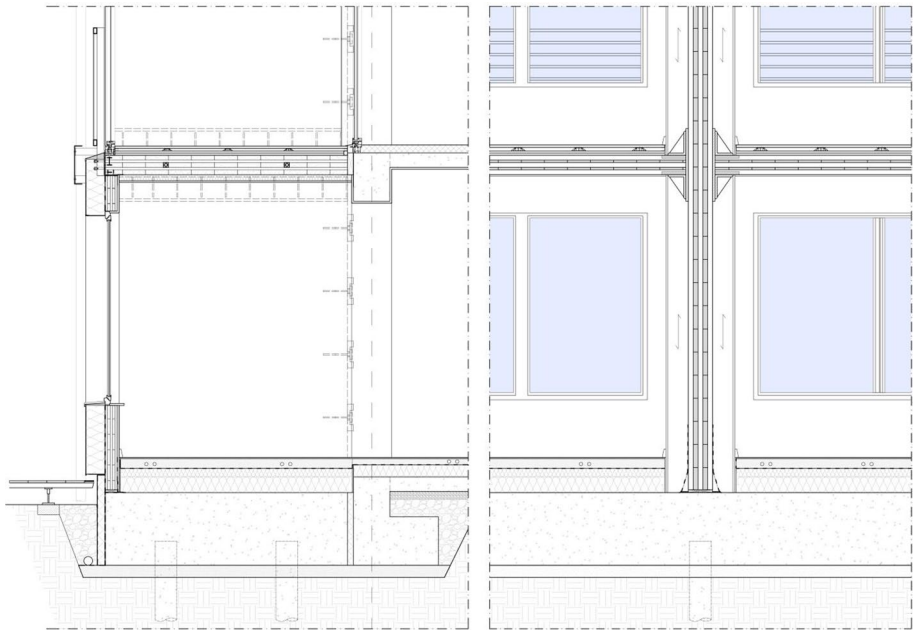


Fig. 16 Vertical and horizontal cross-section details of the foundation system hypothesized for the Brasov case study with the timber-based integrated system. On the left providing the sunspace scenario and on the right with the extra-room

Fig. 15b. The proposed foundation system was separate from the existing one and involved a 0.8 m thick RC slab over several micro-piles (four per steel shear wall). The steel reinforcement heads of the micro-piles ($\Phi 180/5$ mm) were connected to each other within the plinths with an IPE-profile and reinforced for 1 m at the bottom surface of the RC slabs with spiral bars, in order to avoid local shear failures. The 300 mm diameter micro-piles (considering the outer concrete layer) are then approximately 10 m deep. All the foundation plinths are connected with curbs of the same height of the plinths. Finally, the connection with the steel columns is realised by means of end flanges and anchor bolts (fixed joints).

With difference to the steel exoskeleton, a timber-based solution involves less forces on the ground in terms of vertical compressive loads, but probably resulting in higher vertical tension forces due to a greater susceptibility of the lightweight outer structure to being lifted. It follows that piles or micro-piles will probably be necessary to ensure the seismic strengthening and prevent uplift of the external structure, while the foundation slab and its reinforcement may also be reduced in size, while allowing compactness of the foundation structure, avoiding localised weaknesses at the head of the piles, or at the junction of the connectors with the timber walls (Fig. 16 shows a hypothesised foundation configuration).

The latter were chosen as consolidated strategies to connect CLT walls to the foundation level, even though more practical and efficient solutions could be investigated and proposed to improve the seismic performances of the system and the feasibility. For example, the insertion of steel prestressed cables within the layers of the CLT walls (vertically) could be investigated (Sarti et al. 2016; Van de Kuilen and Xia 2014) to increase the global stiffness,

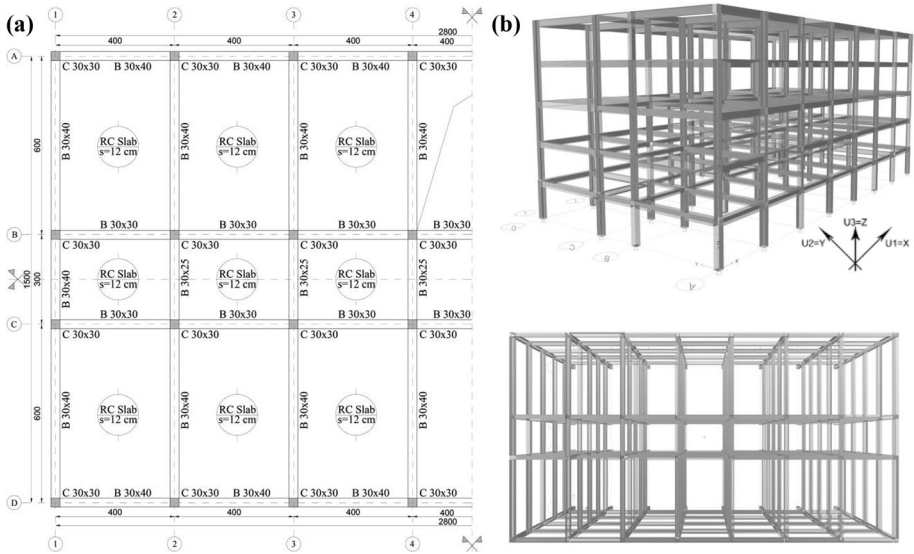


Fig. 17 **a** Typical horizontal cross section of the moment-resisting structure. Due to the symmetry of the structure only half of the planimetry is shown. Cross-sectional dimensions of beams (B) and columns (C) are indicated in cm together with spans; **b** Finite element model of the initial state (reinforced concrete moment-resisting structure)

Table 5 Cross-sectional dimensions of beams (B) and columns (C) are indicated in the table together with the relative reinforcement content and spanning lengths

Cross-section mm	Span m	Long. Rebar		Trans. Rebar φ/step (mm)
		Top	Bottom	
C 350 × 350	2.6	3φ18	3φ18	φ8/200
C 300 × 300	2.6	2φ18	2φ18	φ8/200
B 350 × 400	4	3φ14	3φ14	φ8/200
B 350 × 400	6	2φ18 1φ14	3φ14	φ8/200
B 350 × 250	3	3φ14	3φ14	φ8/200
B 350 × 300	4	3φ14	3φ14	φ8/200
B 300 × 400	4	3φ14	3φ14	φ8/200
B 300 × 400	6	2φ18 1φ14	3φ14	φ8/200
B 300 × 250	3	2φ14	2φ14	φ8/200
B 300 × 300	4	3φ14	2φ14	φ8/200

exploiting the rocking mechanisms and consequently reducing the amount of connectors (hold-downs and angular brackets). As regards as the connection with the existing foundations, specific assessments should be done on every possible case study, considering the morphology, the mechanical characteristics and the status of possible degradation, but it is the author opinion that maintaining separate foundations could simplify the design of the external new structures, always taking into account the possible consequences on the existing foundations in case of removal and modification of the soil surrounding the building.

3 Finite element model

A numerical model was developed with the finite element software ETABS (CSI 2018) both for the existing RC structure alone (initial state — IS) and for the combined solution with the CLT external structure (project state — PS). Through linear dynamic (modal response spectrum) and non-linear static (pushover) analyses, it was subsequently possible to assess the seismic improvement.

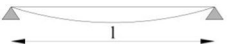
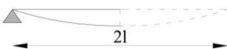

3.1 Initial state: existing structure

The existing moment-resisting RC structure is developed based on the existing case study of Brasov and located in the same area. The structure consists of five floors of 2.6 m height each with a total plan size of 28×15 m measured from the barycentric axes of the frames. The horizontal structures are made of 120 mm thick concrete slabs that can be considered as diaphragm constraints transferring the vertical loads in both the main directions. The beams have different heights depending on the spans, and a width that corresponds to the side of the columns. These vertical elements are 350×350 mm at the ground floor and 300×300 mm for the remaining storeys. The spans between columns are following the morphology of the reference Brasov structure but adapting the dimensions to the different structural system. Along the longitudinal direction (X) the frame presents 7 spans of 4 m, while in the transversal direction (Y) two spans of 6 m are interrupted by a single 3 m span (Fig. 17).

The dimensions of the structural elements and the amount of reinforcement are designed based exclusively on vertical loads, with stresses coming from the ultimate limit state combination as defined by the Eurocodes (CEN 2002, 2004a). The cross-sectional dimension of the structural elements together with the reinforcement content are indicated in Table 5. In addition to dead loads, including weights coming from the various masonry infill and partition walls, live loads referred to residential building were considered. As regards of the materials, concrete class C20/25 ($f_{ck,cyl} = 20$ MPa) and steel grade PC52 ($f_{yk} \geq 355$ MPa) were used with reference to the technical assessment report provided by the municipality of Brasov in the framework of Pro-GET-onE (Maslaev Consulting 2015).

A three-dimensional model was created to carry out the seismic analyses (Fig. 17b). Fixed joints were introduced at the foundation level as external restrains and diaphragm semi-rigid constraints were introduced for all the joints belonging to the floor levels, defined as membranes of 120 mm in RC. Beams and columns were modelled as nonlinear frame elements with lumped plasticity by defining plastic hinges at both ends of the elements. The hinge properties follow the formulas reported in the Annex A of the Eurocode 8-Part 3 (CEN 2005) for ductile mechanisms and can identify the performance levels for each step of the non-linear static analysis (see paragraph 4). The behaviour of these hinges is depending on the cross-section of the element, the material properties, the longitudinal and transversal steel reinforcements, and the axial loads calculated with a quasi-static combination of vertical loads. ETABS provides default-hinge properties, PMM (combined flexural and axial loads) hinges for columns and M3 (only flexural loads) hinges for beams were assigned. In order to take into account brittle failures on the same elements, force-controlled hinges were placed in the middle of each column and at the ends of each beam (V2 for beams and V2-V3 for columns). The shear strength, which is the maximum allowable force for these hinges, is calculated with reference to the paragraph 6.2.3 of (CEN 2004a). As unique difference between the non-linear model and the linear one a

Table 6 Reduction factors imputed on the orthotropic material used in the software to describe the timber layers in the cross-laminated timber elements

Structural element	Static scheme	Reduction factor applied to E of the timber
Horizontal slabs		0.81
Walls at the ground floor		0.89
Walls at the typical floor		0.67

The static schemes used do not take into account the rotational stiffness of the post-tensioned connections in the cases of horizontal slabs and walls in the levels from 1 to 5

consideration was made on the concrete cracking. On this purpose, in the linear model a property modifier is reducing beam and column shear and flexural stiffnesses of 50% as indicated in (CEN 2004c).

3.2 Project state: CLT structure

As mentioned above the CLT walls are placed in the same plane of the RC frames and are increasing the performance against horizontal loads acting in-plane to the walls. In the longitudinal direction, the two systems remain independent. Therefore, to obtain an improvement in both the main directions, the CLT external structure must be provided on the entire perimeter as shown in Fig. 2.

In the numerical model the CLT panels are realised with shell layered elements that provides crossed layers of the implemented timber orthotropic material (CLT made of birch and spruce as defined in Table 1). The correct behaviour of the CLT panels is checked based on (Aondio et al. 2020a, b). Basic FEM models were created to verify the possibility of using shell layered elements as CLT panels. The deformations due to out-of-plane loads, the torsional stiffness, the stability with second order effects and the in-plane shear stiffness were carefully compared with hand-calculations. All these numerical tests gave good results with variations in displacements below the 2% apart for the deformations due to out-of-plane loads. In fact, the shell layered elements follow a Kirchhoff formulation and, as stated in (Aondio et al. 2020a), do not consider the shear rigidity S_{xz} with an error that decreases as the length of the element increases (higher slenderness). Therefore, to take into account the shear deformation, a reduction of the modulus of elasticity is applied at the orthotropic material imputed for the various layers depending on the static scheme of each considered element (see Table 6) as indicated in (Aondio et al. 2020a).

Table 7 Rotational effective elastic stiffness of the post-tensioned cross-laminated timber (PT-CLT) connections referred to 1 m CLT structure

Value	Units	Inner PT-connection	Outer PT-connection
$k_{vert.loads}$	kNm/rad	117'000	23'565
$k_{horiz.loads}$	kNm/rad	13'102	23'565

Table 8 Values of the elastic stiffness of the steel connecting rods ($\phi 12$), single and double angular brackets (type BMF116) (Dujic et al. 2010) and hold downs (type HTT22) (Dujic et al. 2010); friction is neglected in linear analyses

Connector	Units	Tensile strain	Shear strain	Tensile strain	Shear strain
		Single connector (one side)		Double connector (two sides)	
$k_{\phi 12}$	kN/m	158'336	–	–	–
k_{BMF116}	kN/m	5000	8000	10'000	16'000
k_{HTT22}	kN/m	11'250	–	22'500	–

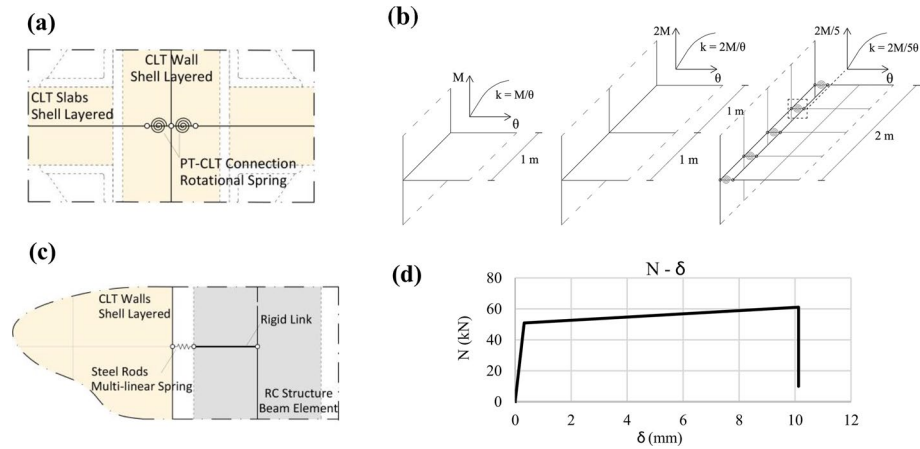


Fig. 18 **a** Finite element modelling (FEM) of the inner post-tensioned cross-laminated timber (PT-CLT) connection; **b** Distribution of the PT-CLT connection in multilinear rotational springs; **c** FEM of the steel fixing rod connection between reinforced concrete columns and CLT walls; **d** Envelope and load bearing capacity of the steel rods applied as axial connectors. While the tensile behaviour is characterised by the tensile capacity of the $\phi 12/150$ rods, the compressive transfer is guaranteed by the hardwood pieces

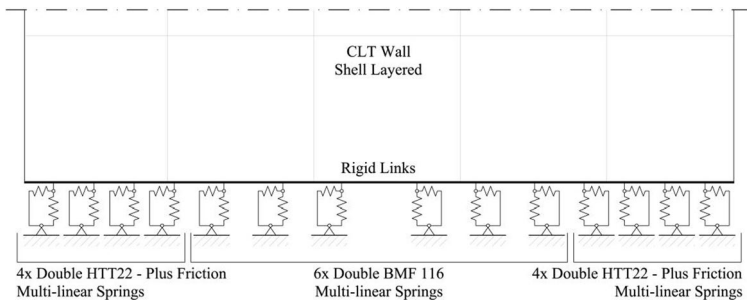


Fig. 19 Finite element modelling of the connectors provided at the base of the shell layered cross-laminated timber wall on one side

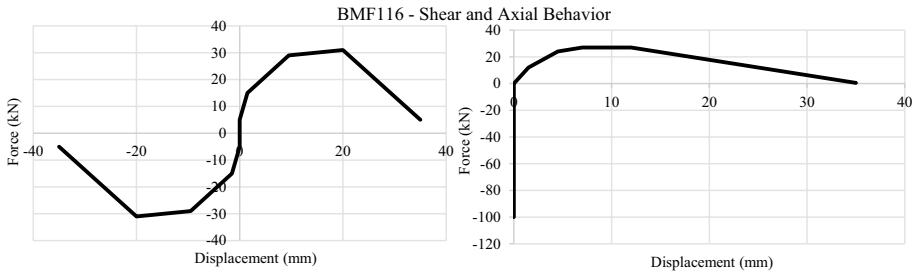


Fig. 20 Envelope and load bearing capacity of the shear anchor with 12 nails of ϕ 4 / 60 mm when acting in shear (left graph) and with axial loads (right graph) (Dujic et al. 2010)

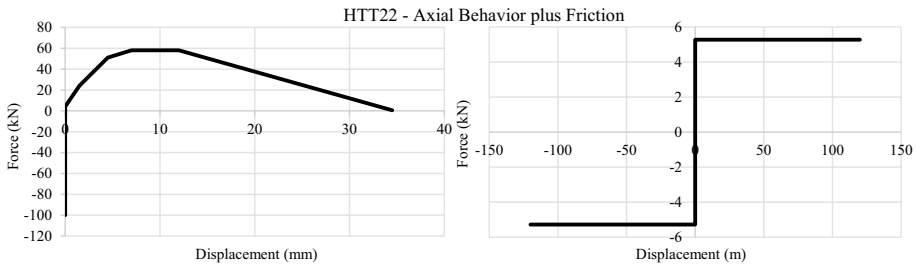


Fig. 21 Envelope and load bearing capacity of the hold-down with 22 nails of ϕ 4 / 60 mm for preventing up-lifting (left graph) and 1/8 of the friction contribution (Dujic et al. 2010)

$$B_{eff,x} = \frac{B_x}{1 + \frac{B_x \cdot \pi^2}{S_{xz} \cdot l^2}} \rightarrow R_F = \frac{B_{eff,x}}{B_x} - reduction\ factor \tag{20}$$

Multi-linear springs with linear stiffness and relative linear and non-linear behavioural laws are implemented in the model to represent the various connectors involved (PT-CLT connections, hold-downs, angular brackets, steel fixating rods) and the activated friction. The PT-CLT connection was implemented in the FEM with rotational springs (Fig. 18a) characterised by the behavioural law (moment-rotation) illustrated in Fig. 8 and a linear stiffness calculated considering the angular coefficient of the line in the elastic phase (Table 7). Since shear deformations were relevant only for horizontal loads, two models were developed independently with PT-CLT connections set respectively for vertical loads (ultimate limit state, ULS and serviceability limit state, SLS) and horizontal loads (significant damage limit state, LS-SD and damage limitation limit state, LS-DL). The 2 m depth shell-layered elements, representing the CLT structural elements, were regularly divided in four parts creating five joints at the edges. The stiffness of each spring (five for each PT-CLT-connection) is determined considering double of the depth of the single 1 m system (multiplying by 2) and then assigning 1/5th to each spring located at the connecting side. In the same way the moment-rotation behaviour is distributed along the rotational springs as shown in Fig. 18b.

The connection with the existing structure is realised in FEM with a multi-linear spring with a linear stiffness as reported in Table 8 and an axial linear and non-linear behaviour as represented in Fig. 18d. Twenty connectors are provided along the height of the entire

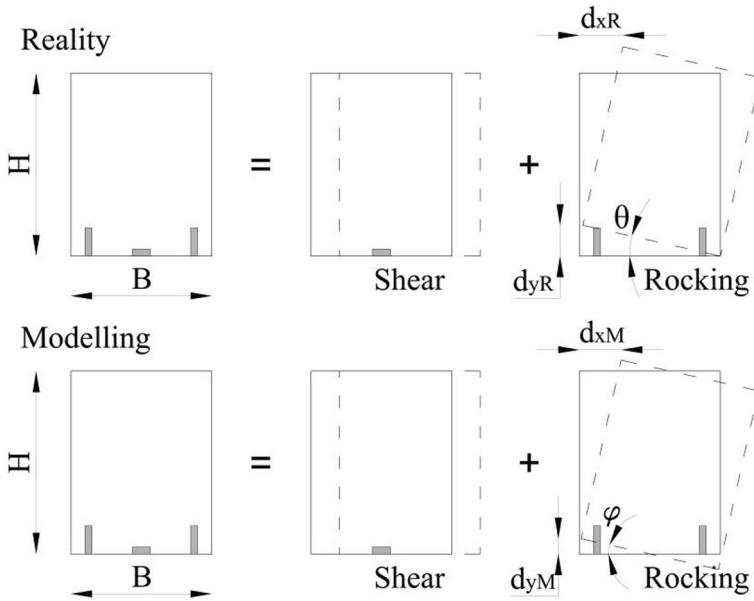


Fig. 22 Connector’s stiffnesses, determination of the axial linear equivalent stiffness to be used in the finite element model

structure (four per storey) and connected to the joints of the CLT-shell elements and to rigid links representing the thickness of the RC columns (Fig. 18c).

Regarding the foundation connectors, a series of rigid links is provided at the final side of the shell layered element to adjust the shell subdivisions with the multi-linear springs representing angular brackets, hold-downs, and friction (Fig. 19). While angular brackets (BMF116) are characterised by behavioural laws describing deformations under axial and shear loads, the hold-downs (HTT22) only present the first component. To simplify the model, the springs representing the hold-downs also contain the friction contribution (divided by the number of springs considered along the length). The envelope and load bearing capacity of these connectors are shown in Figs. 20 and 21 for single connector with reference to (Dujic et al. 2010).

In the FEM, forces and linear stiffnesses of the connectors have been doubled because of a double number of connectors intended to be applied on both sides of the CLT walls.

It is important to mention that for the linear analyses the axial behaviour of the connectors cannot be represented correctly due to actual non-linear behaviour from tension to compression. Therefore, since the deformation in the model is twice the one of a real in-plane loaded CLT wall (considered as rigid body, see Fig. 22), the axial linear stiffness of the connectors has been doubled.

$$d_{yR} = \theta B = \frac{F_{HD}}{k_{HTT22,R}} \tag{21}$$

$$d_{xR} = d_{yR} \frac{H}{B} = F_{HD} \frac{H}{B} \frac{1}{k_{HTT22,R}} \tag{22}$$

Table 9 Results of the modal analysis of the initial and project state of the Brasov MRF; periods are expressed in seconds while participating masses are percentages of the total mass of the building

Mode	Period (s)	Participating mass		
		U1	U2	RZ
Initial state				
1	1.138	0	79.1%	0
2	1.061	79.6%	0	≈ 0
3	0.976	≈ 0	0	79.64%
4	0.364	0	11.1%	0
Project state				
1	0.942	71.0%	0	≈ 0
2	0.890	0	72.5%	0
3	0.847	0	≈ 0*	4.5%*
4	0.847	0	3.2%*	≈ 0*
5	0.802	≈ 0	0	66.4%
6	0.660	6.72%*	0	≈ 0*
7	0.660	≈ 0*	0	5.5%*

*These percentages are linked to vibration modes involving principally the timber-based exoskeleton in displacements unrelated to the RC MRF

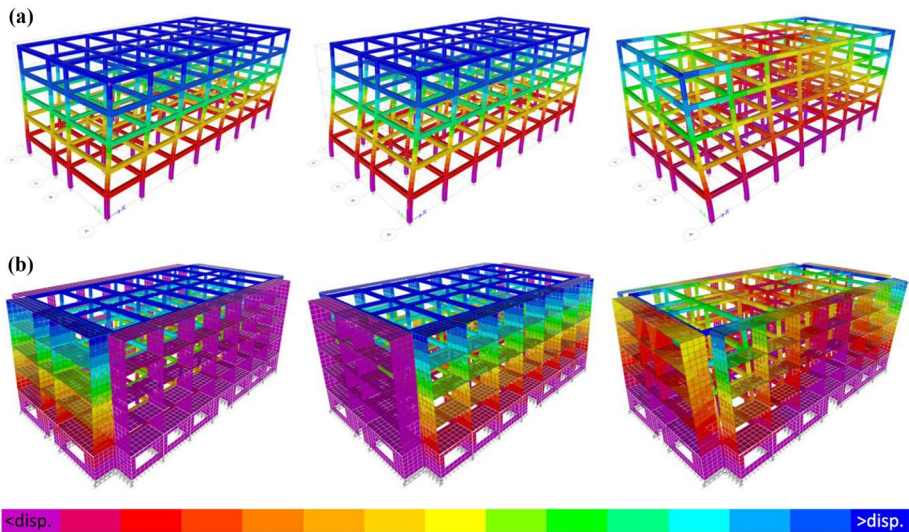


Fig. 23 **a** Representation of the first three main vibration modes in ascending order from left to right; **b** Representation of the first two vibration modes and the fifth one, in ascending order from left to right; the displacements increase from purple to blue

$$d_{yM} = \varphi \frac{B}{2} = \frac{F_{HD}}{k_{HTT22,M}} \tag{23}$$

$$d_{xM} = 2d_{yM} \frac{H}{B} = F_{HD} \frac{H}{B} \frac{2}{k_{HTT22,R}} \tag{24}$$

$$k_{BMF116,R} = k_{BMF116,M} \quad (25)$$

$$2k_{HTT22,R} = k_{HTT22,M} \quad (26)$$

4 Seismic analyses

Modal response spectrum dynamic linear analyses (RSAs) and static non-linear pushover analyses (SPOs) were carried out before and after the application of the timber-based addition on the basis of the provisions of the Eurocode 8 (CEN 2004c). While RSAs were used to design the new structural elements and connections, reporting the stresses affecting them in the different design load combinations (ULS, SLS and LS-SD), SPOs allowed to assess the seismic vulnerability before and after the structural strengthening, thus determining the obtained improvement. These types of seismic reinforcement, because of their size and the impact they have on the existing building, must be accompanied by dynamic analyses to investigate the behaviour of the structural system after the intervention. Guaranteeing their effectiveness and ensuring the absence of induced torsional mechanisms or localised issues. Due to the mechanical nature of the wood material and the characterisation of its connectors, as mentioned in the previous chapter, non-linear analyses would be preferred as they allow the calculation of the non-linearity of materials and connections. It follows that a non-linear dynamic analysis would be optimal in the determination of the behaviour of the structural system post intervention and the actual seismic improvement. The study continued with the non-linear static analysis as it is simpler from a computational point of view and above all in terms of defining the hysteresis cycles of the numerous connections used. By defining these cycles on the behaviour of the connectors, it would have been possible to verify their behaviour over time, even correctly identifying the amount of energy dissipated by each element. The definition of the cyclic behaviour of the connectors, although present in the state of the art, is time consuming and more correctly addressed by appropriate experimental tests on the specific case. The use of pushover analysis implied accepting some simplifications, such as the use of certain horizontal force distributions (not necessarily realistic but suggested by the standards) and the assumption of applying the earthquake action along the two main directions of the building development. On the other hand, it is well known that as the complexity of the analyses decreases, the results in terms of verifications and vulnerability are more conservative, not to mention that the structural regularity of the building in question allows this simplification to be made, possibly assuming that for different directions of application of the horizontal actions, the decomposition of the force in the two main directions would result in the case histories addressed in the following study. Despite the limits of the linear analysis already mentioned, the results of the modal analysis carried out on the initial and design state are reported below, to mention the dynamic aspect of the project.

The analysis was carried out considering the first 12 vibration modes (modal masses greater than 5%) and checking that the total mass activated by the modes is greater than 85%. The following are the results of the first vibration modes for the initial and project state (Table 9). The participating masses (Table 9) and the modal displacements (Fig. 23a) show that the dynamic behaviour of the structure at the initial state is substantially regular,

Table 10 Maximum forces obtained with the response spectrum analysis at the limit state of significant damage for the different components of the connectors: steel connecting rods ($\phi 12$), angular brackets (BMF116) and hold downs (HTT22); the capacities are also reported considering a k_{mod} of 1.1 and a γ_m of 1.3

Value	Units	Maximum design force	Capacities
$N_{\phi 12}$	kN	55.00	61.07
V_{BMF116}	kN	9.32	23.44
N_{BMF116}	kN	7.98	21.62
N_{HTT22_22n}	kN	47.11	46.54
N_{HTT22_26n}	kN	-	55.00

the first two vibration modes act along the main two directions, while the third is torsional. The periods of the structure are relatively high due to the stiffness reduction of the structural elements (present only in the linear analyses) and the dimensions of the column cross-sections.

Table 9 and Fig. 23b show that also for the project state the dynamic behaviour is substantially regular. The first two vibration modes act along the main two directions and the fifth one represents the torsional global component. The release of the timber-based exoskeleton along the longitudinal direction (in parallel with the existing façades) implies the presence of vibration modes involving the masses of the exoskeleton unrelated in terms of natural frequency to the modal displacements of the existing RC moment-resisting structure.

A type 1 elastic response spectrum on ground type A was matched (Fig. 26) with the use of the database provided in (Giardini et al. 2014), characterised by a peak ground acceleration of 0.2 g with a return period of 475 years ($P_r = 10\%$ in 50 years), and then increased with respect to the soil factor B as indicated in the available technical report (Maslaev Consulting 2015). Based on the elastic response spectrum different design spectra were defined depending on the different q-factors, obtained with the SPOs (differentiated by directions and state of the project), and reported in Table 11. The design response spectrum

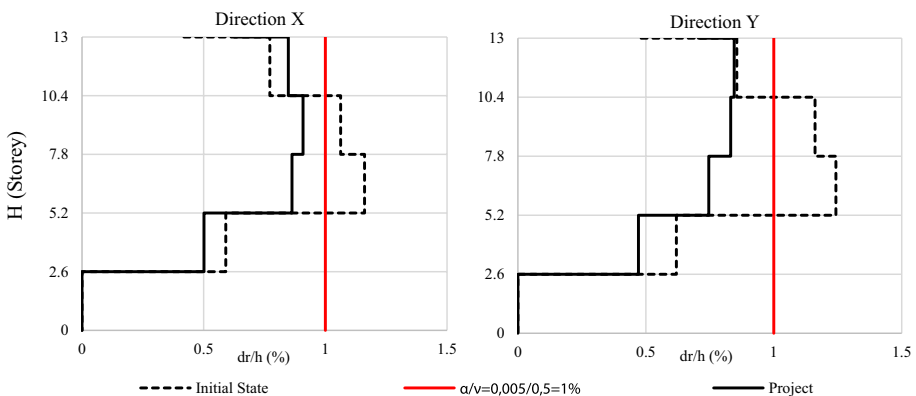


Fig. 24 Interstorey drift verification in both the main directions (X, Y) before and after the project application

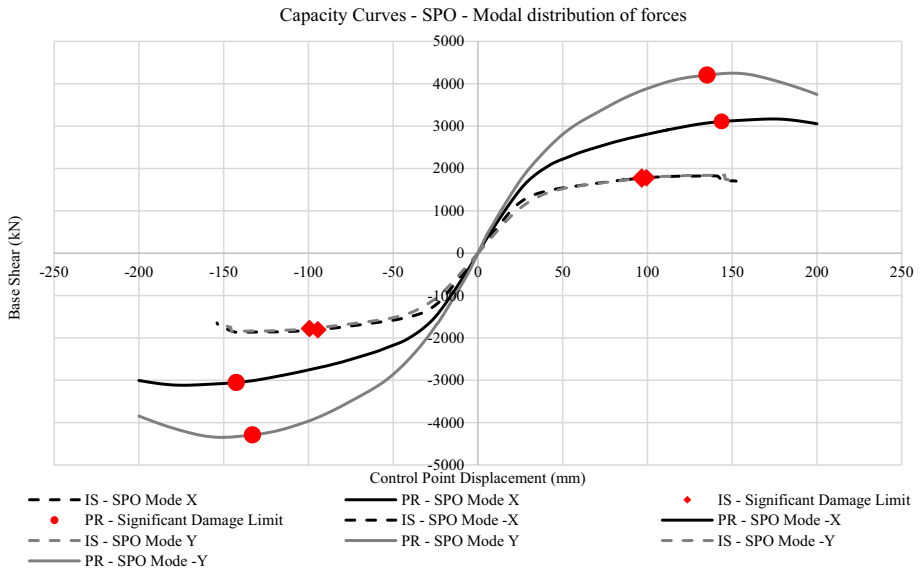


Fig. 25 Capacity curves obtained with the static non-linear pushover analyses proportional to the lateral forces associated with the vibrating modes for both the main directions and signs, before and after the project application

for LS-SD was calculated by dividing the ordinates of the elastic response spectrum by the q-factor. The latter was defined for this case study, following the approach presented in (Maheri et al. 2003). With reference to Table 11, the following values were obtained from the pushover analyses based on the maximum displacement set to the LS-SD (formation of the first plastic hinges beyond the limit state of significant damage).

- R_{μ} ductility reduction factor, defined as the ratio of the elastic design force (V_e) to the yield strength level (V_y), reflecting the energy dissipation capacity of the system and coinciding with the ductility (μ) measured as the ratio of the displacement capacity (Δ_{max}) at the LS-SD to the displacement linked to the yield point and the idealised elastic-perfectly plastic response curve (Δ_y) (Maheri et al. 2003).
- R_s the overstrength factor, defined as the idealised structural yield level (V_y) and the first actual significant yield level (V_s), corresponding to the first hinge beyond the LS-DL (limit state of damage limitation; similar to what defined by the Eurocodes), representing the reserve strength that exists between the two points (Maheri et al. 2003).

The behaviour factor (q) was finally evaluated for this specific case study in Brasov, as product between the ductility reduction factor (R_{μ}) and the overstrength factor (R_s). The minimum q-factors were selected among the analyses performed in both directions. For the initial state 2.90 and 2.67 were used for longitudinal and transversal direction respectively, while a value of 1.50 was always imputed for the verification of brittle mechanisms.

The stresses belonging to the RSAs were combined with a quasi-permanent combination of vertical loads and verified for each CLT panel (slabs and walls) as indicated in (CEN 2004b; Aondio et al. 2020b). Furthermore, also ULS and SLS combinations were checked using, as mentioned in previous paragraphs, two different models based on

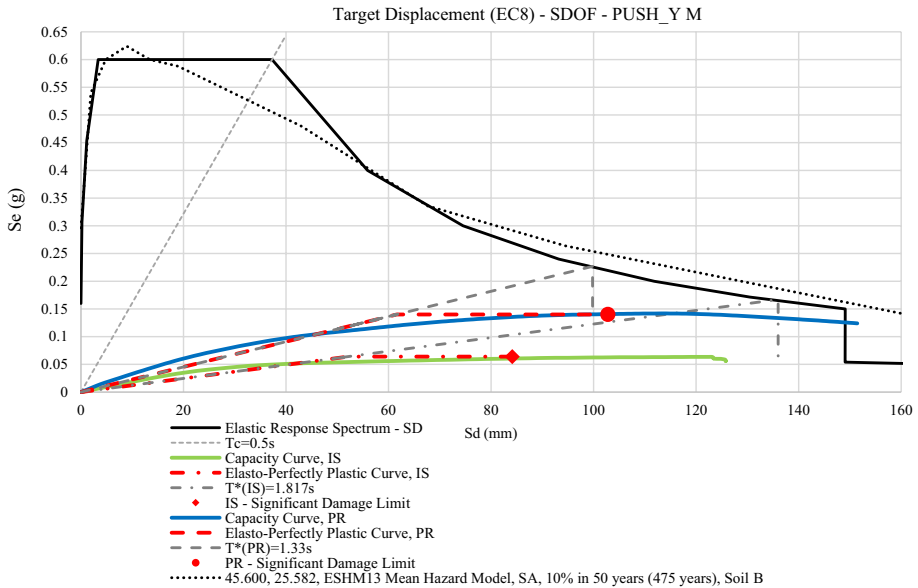


Fig. 26 Pseudo-acceleration and displacement elastic response spectrum (0.2 g), capacity curves of the equivalent single-degree-of-freedom system with associated elasto-perfectly plastic curves and indicating displacement capacities, period values; through T^* and the elastic response spectrum the demanded displacements are also defined. The black dotted line represents the registered elastic response spectrum of Brasov (45.600–25.582), matching continuous line of the EC8 spectrum (CEN 2004c; Giardini et al. 2014), www.efehr.org/Documentation/licenses-copyright

different rotation springs representing the PT-CLT connections. For the verifications, the capacity of the PT-CLT connection was considered with losses in the tendon force about 30% as indicated in (Gräfe et al. 2018; Wanninger 2015; Wanninger et al. 2015). In the same way, all the forces affecting the connectors were checked (hold-downs, angular brackets, PT-CLT connections and steel bars), resulting in the fulfilment of the requirements. The only exception was related to some external hold-downs that would have required an increased number of nails with a consequent increased stiffness and an additional iteration of the design not included in this study. In Table 10 the maximum forces affecting the connectors are shown together with the strength capacity (both with 22 and 26 nails for the axial capacity of the hold-downs).

With the displacements obtained through the RSAs was possible to check the interstorey drift (d_p) before and after the application of the timber strengthening solution for both the main directions following 4.4.3.2 of (CEN 2004c). As shown in Fig. 24, the interstorey drifts of the centres of masses (CM, calculated on the existing building) resulted beyond the design requirements for the initial state and verified in the project solution. Resulting, in terms of capacity/demand ratios, in an improvement from 80 to 110%.

A force controlled static non-linear analysis based on the quasi-permanent vertical loads combination constitutes the starting point for the displacement-control pushover analyses (SPOs). The latter were performed, as required by the standards (CEN 2004c), in both direction, with positive and negative signs and using two different lateral load distributions: proportional to mass regardless of elevation and proportional to the lateral forces associated to the main vibrating modes. As results, capacity curves associating the total

Table 11 Target displacement verification for the significant damage performance level (LS-SD), $T_R=475$ years, $P_V=10\%$ in 50 years

Analyses	Capacity Displ. (mm) Shear (kN)	Demand Displ. (mm) Shear (kN)	C/D (%)	R_μ	R_S	q
SPO X	90.1 2185	126.6 2262	71	1.86	1.66	3.08
SPO -X	88.4 2228	124.6 2307	71	1.84	1.74	3.19
SPO MX	96.7 1773	147.1 1903	66	1.75	1.81	3.17
SPO M-X	99.4 1778	146.5 1894	68	1.70	1.71	2.90
SPO Y	89.2 2181	136.9 2275	65	1.67	1.63	2.72
SPO -Y	85.7 2255	133.5 2352	64	1.63	1.64	2.67
SPO MY	99.4 1778	160.7 2045	62	1.61	1.78	2.88
SPO M-Y	98.7 1774	159.3 2015	62	1.61	1.78	2.88
P-SPO X	129.3 4227	114.3 4142	113	1.91	1.99	3.81
P-SPO -X	127.3 4255	113.1 4184	113	1.89	1.92	3.63
P-SPO MX	143.8 3109	139.1 3091	103	1.84	2.07	3.81
P-SPO M-X	142.5 3053	139.7 3042	102	1.83	2.07	3.79
P-SPO Y	119.9 5337	110.4 5273	109	1.67	1.74	2.90
P-SPO -Y	118.1 5438	109.0 5373	108	1.65	1.72	2.84
P-SPO MY	135.2 4204	131.3 4186	103	1.67	1.86	3.11
P-SPO M-Y	131.7 4192	130.3 4276	101	1.63	1.95	3.18

Capacities and demands are expressed in mm of the control points and related base shear values (kN) for the analyses that regard the initial state (static pushover analysis, SPO) and the project (P-SPO). The letter M indicates the analyses done with lateral load distribution proportional to the main vibrating modes

base shear acting at each loading step with the displacement of the control point, situated in the roof, are derived for the multi degree of freedom (MDOF) model. Below, in Fig. 25, the capacity curves of the structure before and after the application of the timber addition are shown for both the main directions and with the weakest distribution of forces corresponding to the one proportional to modal shapes.

It is possible to notice that the structure in the IS has a comparable behaviour in both directions, while due to the higher number of CLT walls applied along the longitudinal direction, the PS sees increased stiffness and capacity in transversal direction (Y).



Fig. 27 Deformed shapes of the static non-linear pushover analysis in transverse direction (SPO Y) before and after the project application; the coloured dots represent the state of the plastic hinges and indicate for the project solution the achievement of a diffuse collapse mechanism, preferable to a concentrated one. The comparison is made at the step corresponding to the collapse of at least one non-linear hinge of the reinforced concrete structure (red dots), thus implying a different amount of total horizontal forces applied to the system. A displacement of 122 mm and a base force of 1831 kN at the 56th step of the SPO MY are compared with 135 mm and 4122 kN at the 61st step of the P-SPO MY respectively

Table 12 Total horizontal forces registered at the step of the pushover analyses identifying the limit state of significant damage, divided on reinforced concrete and cross-laminated timber components with exploitation percentages of the external strengthening solution

Analyses	Total (kN)	RC (kN)	CLT (kN)	%
P-SPO X	4145	2597	1548	37
P-SPO MX	3108	2573	535	17
P-SPO Y	5284	3292	1991	38
P-SPO MY	4204	3253	951	23

Furthermore, an increased displacement capacity is recorded as a consequence of the reduction of shear loads concentrated in the lower storeys.

Finally, by using the target displacement verification (TDV) as defined in the Annex B of (CEN 2004c), the displacement capacity is evaluated for which the performance level of significant damage limit state was exceeded for the elements of the existing RC structure. The target displacement is found with the scaled capacity curves representing the equivalent single degree of freedom (SDOF) system and the elastic response spectrum of the site for the LS-SD. In Fig. 26 a comparison between IS and PS is shown, displaying the capacity and demand values for the modal distribution of forces in transversal directions Y (positive sign). Considering the elastic response spectrum introduced above, it was possible to evaluate the ratio between capacity and demand for all the assessed combination, obtaining an improvement that goes, in the weakest lateral load distribution (modal force distribution), from 62 to 101% in transversal direction (Y), and from 66 to 102% in the longitudinal one (X).

The application of the timber external structure made it possible to increase the q-factors in both directions thanks to a better distribution of the damage along the height of the existing structure. In fact, the RC moment resisting frames present greater deformations in the lower storeys, implying a collapse that does not allow to exploit the full capacity of the RC

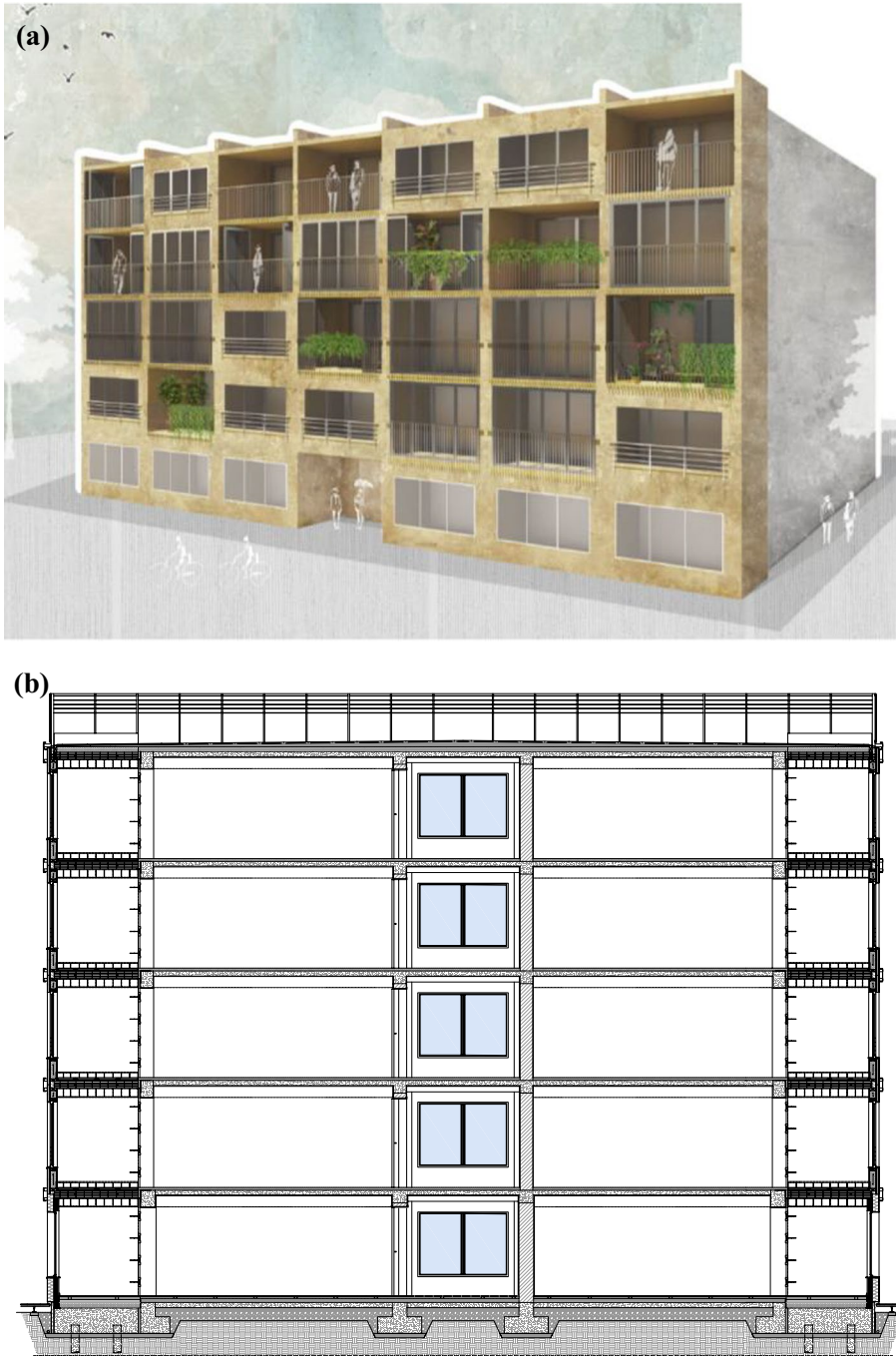


Fig. 28 **a** Representative external view of the applied timber extension with the elevation development of the Brasov case study (Froli 2021); **b** Vertical cross-section of the project state considering the only extra-room as architectural extension units

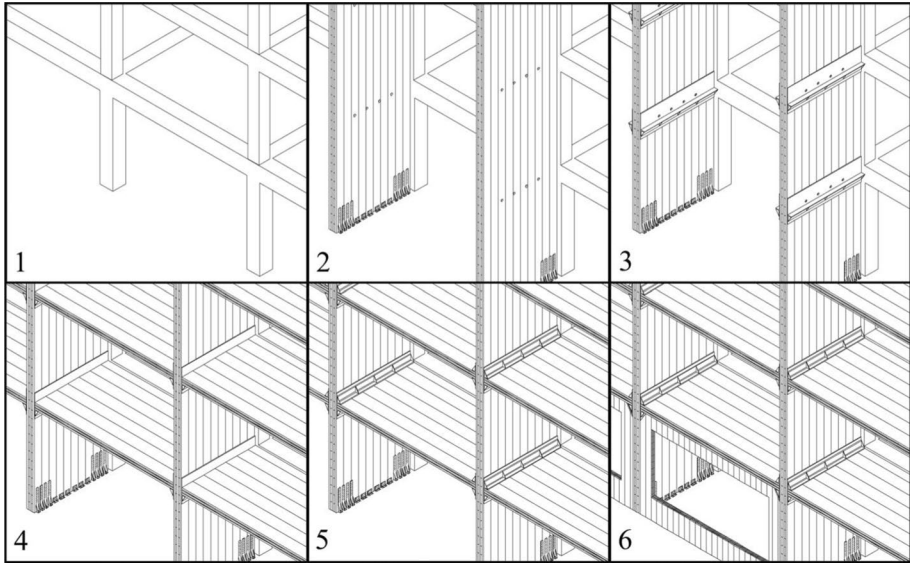


Fig. 29 Sketches representing the steps of the assembly procedure of the structure

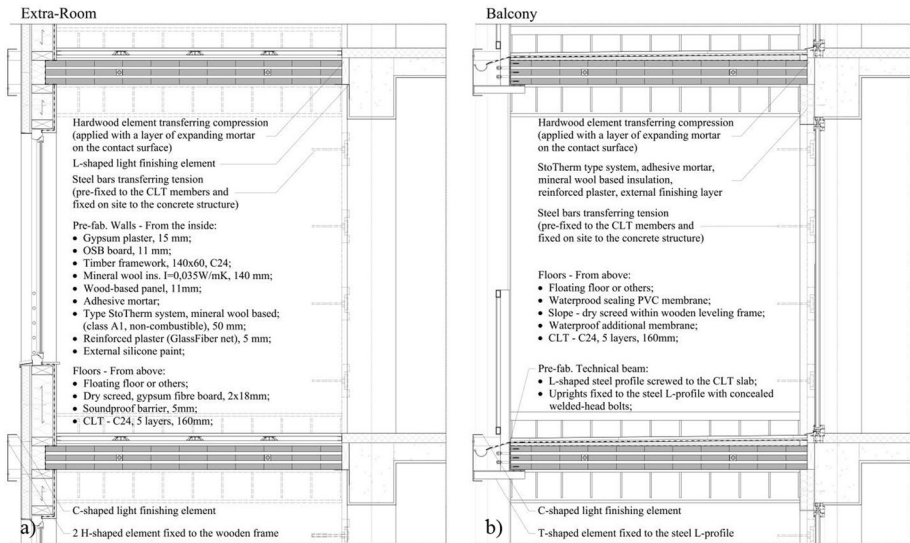


Fig. 30 **a** The detail of the extra-room architectural solution provided within the external cross-laminated timber (CLT) strengthening structure. The prefabricated timber-based walls, providing window frames are easily inserted in between the CLT slabs and fixed to the main structure from the front; **b** The balcony solution provides a technical prefabricated beam fixed to the front side of the CLT slabs

structure (fib 2003; Feroldi et al. 2014). through the application of the timber-based exo-skeleton, higher displacement capacities can be reached due to a modified deformed shape

Table 13 Conductivity values associated to the external vertical partitions, designed to stay below the limit value of 0.24 W/m²K

Walls	Positioning	U (W/m ² K)
Prefabricated timber-based walls	Extra-room	0.196
Insulated RC frames	Balcony and Sunspace	0.232
Insulated masonry infills	Balcony and Sunspace	0.155

of the existing structure. The q-factor values passed from 2.90 to 3.63 for the longitudinal direction (X), and from 2.67 to 2.90 for the transverse direction (Y).

As shown in Table 11, all the seismic analyses resulted satisfied in the project solution. The effect of the application of the strengthening structure on the existing RC moment-resisting frame is shown in Fig. 27, where a uniform shear deformation occurs over the entire height of the building; while previously, the first floors were primarily loaded. Consequently, the existing RC structure before the strengthening intervention faced the collapse of its ground level members a lower level of horizontal forces than the project situation. This translates in terms of global behaviour into lower displacement capacities of the existing structure before the intervention, which are not sufficient to satisfy the displacement demand, implying the failure of the structure for low-intensity seismic events. Particular attention must be paid to the scale of the structural members, since the different deformed shape may determine a different distribution of damage along the height of the building, which on the one hand may be advantageous for the overall performance of the building, while on the other hand determines higher demands for structural elements that were not even affected by deformations before.

Finally, to measure the exploitation of the external structure the amounts of horizontal force taken by both the RC and the CLT structures were derived for the SPOs at the step of the LS-SD (Table 12) highlighting a margin of improvement of the system that could be explored in further steps by varying the base connection system.

5 Technological solutions

The technological solutions were designed based on the objectives of Pro-GET-onE, optimising the pre-fabrication of the components and the assembly procedure, guaranteeing efficient energy performance with a user-oriented approach.

- **Additional space:** the addition of the new housing units is foreseen by the extension through the exoskeleton and could be combined with the new distribution of the internal spaces.
- **Thermal comfort:** through an adequate HVAC system including the renovation of systems inside and/or outside the building envelope (aspect not covered in this study).
- **Safety:** through an adequate strengthening structure to improve the seismic performance of the existing building (previous chapters).

The flexibility of the technique is also determined by the use of different materials depending on the climate or the needs and possibility of the users and owners. Given the need to enhance the environmental sustainability, increasing the amount of CO₂ stored, and decreasing gas emissions with efficient envelopes, technical systems, and renewable resources. The use of the wood-based component applied to the CLT-structure allowed a homogeneity of materials linked to advantages in terms of costs, time, and construction procedures, without mentioning the considerable reduction of environmental impacts. Wood allows a high degree of prefabrication, speeding up the assembly phase and being easy to transport and to manage due to its low weight. The design envisages extensions for each existing room, combining the exoskeleton structure with the existing one, creating new spaces with different uses (Fig. 28). The extension will have a depth of 2 m and can be divided into three main uses: balcony, sunspace, and extra-room. The technological components that create these units represent the main challenge for the architectural design and are mentioned in the this sections.

Thanks to the use of prefabricated wooden elements and post-tensioned connections the assembly procedure of the structure is designed to be fast and practical. The steel connection plates constitute a useful temporary support for the slabs until application of the tension and the lightness of timber means reduction of time and costs.

In order, as shown in Fig. 29:

- CLT walls are fixed to the foundations (suitably designed based on the morphology of the existing ones, design loads and soil condition);
- steel plates without the upper angle profile and providing steel pipes as shear keys are inserted in specific holes in the CLT walls;
- horizontal CLT slabs are lifted on top of the steel L-shaped profiles;
- cables are inserted and the steel composite plate closed with the upper L-profile;
- the entire system is tensioned and the CLT panels at the ground floor are installed;
- after the CLT portals have been tensioned, the prefabricated architectural components (façade panels or technical beams) can be applied to the outer side of the exoskeleton.

It is important to underline again the disruption that could be generated during the construction of the foundations and the application of the connectors to the existing RC columns that could be related to a local strengthening. Subsequently three architectural solutions are provided in direct collaboration with the CLT panels, extra-room (Fig. 30a), sunspace, and balcony (Fig. 30b). For each solution, the design guarantees thermal conductivity performances (U-value) suitable for a nearly zero energy building (Table 13). Pre-assembled façade components are therefore provided: an external wooden frame insulated panel for the extra-room and a technical beam integrated with railings, stringcourse and gutter for balcony and sunspace. In the last two cases, the new envelope is provided on the existing surface and can be easily installed exploiting the external structure.

As regards as fire safety design, no specific studies have been carried on. Depending on local standards, the buildings are classified in type of construction, level of protection needed and degree of protections between parts of the building with or without different purposes. This results in a compartmentalisation that could involve the structural members of the extensions (depending on their living usage) and implying requirements in terms of floors, walls, and connections fire resistance. Usually, the fire resistance is presented as a duration of time and involves load bearing capacity (R), integrity (E) and insulation (I), hence the acronym REI with reference to European terminology. In particular, looking at the proposed project, high level of fire resistances may be reached for

CLT walls and slabs, simply considering the layers of gypsum boards provided in front of the steel composed plates as false walls and ceilings. These layers would not only act as protection system for the timber elements (already efficient considering number and thickness of the crossed lamellas), but also for the steel components, that represents the weakest point for the whole structural system (the Eurocodes indicate that unprotected connections will only achieve a fire resistance period of between 15 and 20 min). Specific attention must therefore be paid to protecting the connections, possibly not only by using gypsum boards against the wall but, if necessary, by using special sprayed plaster. Further studies are needed on this topic, especially with reference to the post-tensioned connection and the effects of temperature increase on the prestressing of the system.

It is important to mention two main problems encountered in the renovation strategy adopted. Both also concern the steel-based solutions, although they have become more evident in the current feasibility study.

The first one concerns the reduction of light inside the existing units, here more relevant due to the massive opacity of the side walls of the wooden portals. In this regard the same feasibility study was investigated at the University of Bologna by a master student (Zucchini 2020), reporting different results in term of spatial daylight autonomy (sDA) and annual sunlight exposure (ASE). A substantial distinction emerged between north and south environments when it comes to natural light. On the north side, no room has a level considered sufficient for sDA, while it always has acceptable levels of ASE. The south side, on the other hand, showed that most rooms have good lighting, often with very high values especially for the top floors. The ASE parameter, however, was often reported to be out of the limit. The large gap between the two sides underlined the need to apply different interventions, dividing the project according to the geographic orientation. While shading devices were required for the south side for an extension depth of 1.2 m, on the north sides they could be avoided and replaced with other devices in order to let in more sunlight. The exploitation of devices that distribute light from the front openings, such as light shelves (Kontadakis et al. 2018) or from the roof as solar tubes, could mitigate this problem.

The second problem depends on the case study and its usable height. Characteristic of this case study, and of many similar residential buildings stock, is the limited interstorey height, often defined in order to comply with the minimum usable height required by regulations by virtue of an optimised design. Consequently, when the height of the structural existing slab (RC) is lower than the thickness of the structural extension (CLT), there will be a decrease of this height. To minimise this problem, it is therefore necessary to at least standardise the architectural solutions adopted for each façade, avoiding the installation of insulation on each additional floor, and closing the heated cores either outside the extension (all extra-rooms) or on the edge of the existing façades (variable balcony or sunspace). It is therefore evident that the possibility of providing user-oriented solutions clashes with the boundaries of standard and hygiene requirements of liveable residential spaces. This issue is strictly dependent on the morphology of the existing building and needs to be addressed either by specific exemptions for the application of the innovative technology, perhaps by imposing more stringent requirements in terms of forced or natural ventilation of rooms, or by changing the renovation strategy.

Finally, it is not always possible to overcome either building regulations or restriction lines that could limit or even eliminate the surface possibly dedicated to extensions. These final requirements constitute mandatory boundaries and should therefore drive the choice of renovation typology at an early stage.

6 Conclusions

The contribution aims to introduce and describe a new integrated technology made out of timber engineering products (CLT panels) to ensure an energy and architectural retrofitting connected at the same time to a structural improvement. It has been proven to be able to answer the three main requirements of the European project Pro-GET-onE, providing an efficient and more sustainable alternative to the more established steel exoskeletons.

To exploit the geometry of the addition maintaining architectural freedom and speeding up the assembly procedure a PT connection between CLT panels is provided through an adaptation of the analytical method proposed in (Wanninger and Frangi 2014). An experimental campaign was carried out on this topic at the Technical University of Munich and some findings are presented here. A conservative response in terms of moment capacity and initial stiffness was obtained by considering mean moduli provided by the manufacturers and low values of tendon forces, showing that the analytical model is able to predict the behaviour of the PT-CLT connection and to allow the implementation of the moment-rotation behaviour in the FEM model.

FEM of the structures were provided for the initial state and for the project solution to verify the new structural elements and to assess the seismic improvement obtained on a RC moment-resisting structure located in Brasov (Romania), and therefore subjected to medium level of seismic hazard (PGA of 0.2 g). The results of the analyses shown that this timber-based external structure could be comparable to a steel exoskeleton (Badini et al. 2019), even though the case study was different, satisfying the design displacement values associated to the performance level of significant damage. The ratio between capacity and demand for all the assessed combination resulted satisfied, obtaining an improvement that goes, considering the weakest lateral load distribution from 62 to 101% in transversal direction (Y), and from 66 to 102% in the longitudinal one (X). Furthermore, verifications for the limit state of damage limitation, in terms of interstorey drifts got satisfied after the application of the integrated system. Resulting, in terms of capacity/demand ratios, in an improvement from 80 to 110%. However, the horizontal forces derived from the capacity curves at performance level of significant damage indicated that globally the CLT walls take from 17 to 38% from the total amount, showing margins of improvement for further steps. In order to increase the global stiffness and consequently improving the performance against frequent earthquakes, the insertion of steel prestressed cables within the layers of the CLT walls (vertically) could be investigated (Sarti et al. 2016; Van de Kuilen and Xia 2014). An increased stiffness at the foundation interface between the CLT walls and the concrete could then be provided exploiting the rocking mechanisms, with a consequent reduction of connectors (hold-downs and angular brackets). Additionally, the insertion of dissipative devices at the level of the connections with the existing structure could decrease the global seismic demand. The current selection of connectors was, in fact, intended to minimise the variables in the numerical analyses. Together with a better selection of the connection strategies, a deeper definition of their behaviour is necessary in order to demonstrate the effectiveness of the strengthening system with non-linear dynamic analysis, which would allow to capture unexpected and cyclic behaviour during seismic events accurately represented by ground motions. Finally, the replicability of the system on different and less regular existing buildings should be investigated, also considering cases where the available space does not necessarily include the whole perimeter and possibly varying the locations of the building, testing higher seismic hazard levels.

A rapid assembly procedure concerning the structure is shown to underline advantages of using lightweight timber products, with respect to steel or concrete counterparts, and the level of prefabrication of the various elements with a consequent optimization of construction time. With the same logic prefabricated technological architectural solutions constitute the finishing “layer” of the renovation, providing an efficient energetic envelope and three possibilities of spacing units.

Acknowledgements This article is part of the Pro-GET-onE project which has received funding from the European Union’s Horizon 2020 Innovation action under Grant Agreement No 723747.

Funding Open Access funding enabled and organized by Projekt DEAL.

Declarations

Competing interest The authors have not disclosed any competing interests.

Open Access This article is licensed under a Creative Commons Attribution 4.0 International License, which permits use, sharing, adaptation, distribution and reproduction in any medium or format, as long as you give appropriate credit to the original author(s) and the source, provide a link to the Creative Commons licence, and indicate if changes were made. The images or other third party material in this article are included in the article’s Creative Commons licence, unless indicated otherwise in a credit line to the material. If material is not included in the article’s Creative Commons licence and your intended use is not permitted by statutory regulation or exceeds the permitted use, you will need to obtain permission directly from the copyright holder. To view a copy of this licence, visit <http://creativecommons.org/licenses/by/4.0/>.

References

- Aondio P, Glaser P, Kreuzinger H (2020a) FE-Berechnung von geklebtem brettsperrholz - Teil 2: Beispiele (German title). *Bauingenieur* 95 (German title)(2):4
- Aondio P, Glaser P, Kreuzinger H, Aondio PGP, Kreuzinger H (2020b) FE-Berechnung von geklebtem brettsperrholz - Teil 1: Theorie (German title). *Bauingenieur* 95 (German title)(1):4
- Assimakopoulos M-N, De Masi RF, Papadaki D, Ruggiero S, Vanoli GP (2018) Energy audit and performance optimization of a residential university building in heating dominated climates of italian back-country *TEMA* 4, n° Special Issue:15
- Badini L, De Stefano CA, Custodi A, Predari G, Ferrante A (2019) Seismic strengthening of existing RC structure through external 3D exoskeleton. In: IABSE congress, New York City, 2019, ed. IABSE. New York, pp 1018–1024
- Barmpareos N, Papadaki D, Karalis M, Fameliari K, Assimakopoulos MN (2019) In situ measurements of energy consumption and indoor environmental quality of a pre-retrofitted student dormitory in athens. *Energies* 12(11):2210
- BBV Systems, Post-tensioning systems. www.bbv-systems.com
- CSI (2018) ETABS ultimate v17.0.1. Integrated building design software. Computers & Structures Inc., Berkeley
- Dangel U (2018) “Tall wood buildings: design, construction, and performance” by michael green and jim taggart. *Technol Archit Des* 2(2):254–256
- Dujic B, Assistant T, Zarnić R (2008) Shear capacity of cross-laminated wooden walls
- Dujic B, Pirmanšek K, Zarnić R, Ceccotti A (2010) Prediction of dynamic response of a 7-storey massive XLAM wooden building tested on a shaking table. In: World conference on timber engineering
- European Committee for Standardization (CEN) (2002) EN 1991-1-1: Eurocode 1: actions on structures—part 1-1: General actions—densities, self-weight, imposed loads for buildings. Brussels, Belgium
- European Committee for Standardization (CEN) (2004a) EN 1992-1-1: Eurocode 2: design of concrete structures—part 1-1: General rules and rules for buildings. Brussels, Belgium
- European Committee for Standardization (CEN) (2004b) EN 1995-1-1: Eurocode 5: design of timber structures—part 1-1: general—common rules and rules for buildings. Brussels, Belgium

- European Committee for Standardization (CEN) (2004c) EN 1998-1: Eurocode 8: design of structures for earthquake resistance—part 1: general rules, seismic actions and rules for buildings. Brussels, Belgium
- European Committee for Standardization (CEN) (2005) EN 1998-3: Eurocode 8: design of structures for earthquake resistance—part 3: assessment and retrofitting of buildings. Brussels, Belgium
- Fédération internationale du béton (fib), Seismic Assessment and Retrofit of Reinforced Concrete Buildings: State-of-the-art report. International Federation for Structural Concrete (fib), Lausanne, Switzerland, 2003. ISSN 1562-3610
- Feroldi F et al (2014) Miglioramento e adeguamento sismico di edifici contemporanei mediante approccio integrato energetico, architettonico e strutturale con soluzioni a doppio involucro a minimo impatto ambientale (Italian title). *Progettazione Sismica (Italian title)* 5:31–47. <https://doi.org/10.7414/PS.5.2.31-47>
- Ferrante A, Fotopoulou A, Semprini G, Cantelli D, Ruggiero S, Karalis M, Efthymiou C, Papadaki D, Assimakopoulos M-N (2019) IEQ and energy improvement of existing buildings by prefabricated facade additions: the case of a student house in athens, 042047
- Ferrante A, Mochi G, Predari G, Badini L, Fotopoulou A, Gulli R, Semprini G (2018) A European project for safer and energy efficient buildings: Pro-GET-onE (proactive synergy of integrated efficient technologies on buildings' envelopes). *Sustainability* 10(3):812
- Fotopoulou A, Badini L, Mochi G, Predari G, Rojakkers R, Cojocar R (2018) Seismic strengthening through external exoskeleton. *TEMA* 4, n° Special Issue:18
- Fotopoulou A, Ferrante A, Badini L, Predari G, Mochi G, Semprini G, Gulli R, Assimakopoulos M, Papadaki D (2019) An integrated system for façade additions combining safe, energy efficient and user-oriented solutions. *TEMA* 5(1):72–81
- Franceschini M, Semproli P, Secci A (2014) I segni della ricostruzione post terremoto maggio 2012: l'adeguamento sismico della palazzina uffici nello stabilimento Magneti Marelli di Crevalcure (Italian title). Inarcos, Ingegneri Architetti Costruttori (Italian title). http://www.teleios-ing.it/UserFiles/File/FRANCESCHINI/Articolo-Inarcos738_Ricostruzione%20terremoto%202012_Franceschini-Semproli-Secci.pdf
- Froli MS (2021) Analysis of the expansion of a building using a modular system in CLT panels. Evaluation of the architectural variability and environmental impact of the moduls. Single Cycle Degree/Combined Bachelor and Master in Architecture and Building Engineering, Department of Architecture, University of Pisa, Pisa
- Gavric I, Fragiocomo M, Ceccotti A (2015) Cyclic behaviour of typical metal connectors for cross-laminated (CLT) structures. *Mater Struct* 48(6):1841–1857
- Giardini D, Woessner J, Danciu L (2014) Mapping europe's seismic hazard. *EOS Trans Am Geophys Union* 95:261–262
- Google LLC, "Street view—August 2012—Google Maps", © 2022 Google. maps.google.com. Accessed 28 Feb 2022
- Granello G, Palermo A, Pampanin S, Pei S, Lindt JVD (2020) Pres-lam buildings: state-of-the-art. *J Struct Eng* 146(6):04020085
- Gräfe M, Dietsch P, Winter S (2018) CLT under in-plane loads: Investigation on stress distribution and creep
- Guardigli L, Bragadin MA, Ferrante A, Gulli R (2019a) Life cycle analysis and planning in the renovation process of public housing. *TEMA* 5(2):14
- Guardigli L, Ferrer C, Peters C, Fotopoulou A, Bragadin MA, Ferrante A (2019b) Rehabilitation of public housing buildings in a life cycle perspective, p 012038
- Hristovski V, Dujic B, Naumovski N, Garevski M (2018) Shaking-table tests and comparative numerical investigation of various upgrade systems on existing RC structures
- Jeitler G, Augustin M, Schickhofer G (2016) Birch GLT&CLT: mechanical properties of glued laminated timber and cross laminated timber produced with the wood species birch. In: WCTE 2016—world conference on timber engineering
- Kontadakis A, Tsangrassoulis A, Doulos L, Zerefos S (2018) A review of light shelf designs for daylight environments. *Sustainability* 10(1):71
- Latke F, Larsen K, Ott S, Cronhjort Y (2011) Tes energy façade—prefabricated timber based building system for improving the energy efficiency of the building envelope, funded by: Woodwisdom net, research project from 2008–2009.
- Maheri MR, Kousari R, Razazan M (2003) Pushover tests on steel X-braced and knee-braced RC frames. *Eng Struct* 25(13):1697–1705. [https://doi.org/10.1016/S0141-0296\(03\)00150-0](https://doi.org/10.1016/S0141-0296(03)00150-0)
- Margani G, Evola G, Tardo C, Marino EM (2020) Energy, seismic, and architectural renovation of RC framed buildings with prefabricated timber panels. *Sustainability* 12(12):4845

- Maslaev Consulting (2015) Technical assessment report - civil engineering works regarding the change of destination from dormitory to community housing: Str. Zizinului no. 126c, Brasov, Romania. Civil engineering works regarding the change of destination from dormitory to community housing. Brasov, Romania
- Mora TD, Righi A, Peron F, Romagnoni P (2015) Functional, energy and seismic retrofitting in existing building: An innovative system based on XLAM technology. *Energy Procedia* 82:486–492
- Ott S, Krechel M (2018) Construction principles of seismic and energy renovation systems for existing buildings. *TEMA 4*, n° Special Issue:15
- Palermo A, Pampanin S, Buchanan AH, Newcombe MP (2005) Seismic design of multi-storey buildings using laminated veneer lumber (LVL)
- Pihelo P, Kalamees T, Kuusk K (2017) NZEB renovation with prefabricated modular panels. *Energy Procedia* 132:1006–1011
- Priestley M, Sriharan S, Conley J, Pampanin S (1999) Preliminary results and conclusions from the press five-story precast concrete test building. *PCI J* 44:42–67
- Pro-GET-onE Consortium (NKUA, ABT and UNIBO) (2018) D2.6: sheets on technical data on the case studies. In: Proactive synergy of integrated Efficient Technologies on buildings' Envelopes: Pro-GET-onE
- Sarti F, Palermo A, Pampanin S (2016) Quasi-static cyclic testing of two-thirds scale unbonded post-tensioned rocking dissipative timber walls. *J Struct Eng* 142(4):E4015005
- Stazi F, Serpilli M, Maracchini G, Pavone A (2019) An experimental and numerical study on CLT panels used as infill shear walls for RC buildings retrofit. *Constr Build Mater* 211:605–616
- Sustersic I, Dujic B (2012) Seismic strengthening of existing buildings with cross laminated timber panels. Paper presentat at the world conference on timber engineering 2012, WCTE
- Sustersic I, Dujic B (2013) Seismic strengthening of existing URM and RC structures using XLAM timber panels
- Sustersic I, Dujic B (2014a). Seismic shaking table testing of a reinforced concrete frame with masonry infill strengthened with cross laminated timber panels
- Sustersic I, Dujic B (2014b) Seismic strengthening of existing concrete and masonry buildings with crosslam timber panels. Springer, Dordrecht, pp 713–723
- Sustersic I, Dujic B, Gostič S (2010) Timber upgrade of structures on seismically active areas
- Sustersic I, Fragiaco M, Dujic B (2016) Seismic analysis of cross-laminated multistory timber buildings using code-prescribed methods: influence of panel size, connection ductility, and schematization. *J Struct Eng* 142(4):E4015012
- Van De Kuilen JWG, Xia Z (2014) Lateral behavior of post-tensioned cross laminated timber walls using finite element analysis. Paper presentat at the WCTE 2014: proceedings of the world conference on timber engineering, Quebec, Canada, 10–14 August 2014, 2014-08-10
- Wanninger F (2015) Post-tensioned timber frame structures. Doctoral Thesis
- Wanninger F (2017) Fast assembled post-tensioned timber frames. Paper presentat at the 7e Forum International Bois Construction, FBC 2017
- Wanninger F, Frangi A (2014) Experimental and analytical analysis of a post-tensioned timber connection under gravity loads. *Eng Struct* 70:117–129
- Wanninger F, Frangi A (2016) Experimental and analytical analysis of a post-tensioned timber frame under horizontal loads. *Eng Struct* 113:16–25
- Wanninger F, Frangi A, Fragiaco M (2015) Long-term behavior of posttensioned timber connections. *J Struct Eng* 141(6):04014155
- Zucchini F (2020) Progetto di un nuovo involucro nel caso di un edificio a Brasov (Italian title). Single Cycle Degree/Combined Bachelor and Master in Architecture and Building Engineering Master Thesis, Department of Architecture, University of Bologna - Alma Mater Studiorum, Bologna, 2020

Authors and Affiliations

Lorenzo Badini^{1,2}  · Stephan Ott¹  · Patrik Aondio¹  · Stefan Winter¹ 

Lorenzo Badini
lorenzo.badini@tum.de; lorenzo.badini3@unibo.it

Stephan Ott
ott@tum.de

Stefan Winter
winter@tum.de

¹ Chair of Timber Structures and Building Construction, Technical University of Munich, Arcistraße 21, 80333 Munich, Germany

² Department of Architecture, University of Bologna, Bologna, Italy